

Universal Homoclinic Bifurcations and Chaos near Double Resonances

G. Haller¹

Received February 14, 1995; final August 30, 1996

We study the dynamics near the intersection of a weaker and a stronger resonance in n -degree-of-freedom, nearly integrable Hamiltonian systems. For a truncated normal form we show the existence of $(n-2)$ -dimensional hyperbolic invariant tori whose whiskers intersect in *multipulse* homoclinic orbits with large splitting angles. The homoclinic orbits are doubly asymptotic to solutions that “diffuse” across the weak resonance along the strong resonance. We derive a universal *homoclinic tree* that describes the bifurcations of these orbits, which are shown to survive in the full normal form. We illustrate our results on a three-degree-of-freedom mechanical system.

KEY WORDS: Hamiltonian systems; resonances; homoclinic bifurcations; chaos.

1. INTRODUCTION

This paper is concerned with Hamiltonian systems of the form

$$H(I, \phi; \varepsilon) = H_0(I) + \varepsilon H_1(I, \phi; \varepsilon) \quad (1)$$

where $(I, \phi) \in \mathbb{R}^n$ are n -dimensional action-angle variables, $0 < \varepsilon \ll 1$ is a small perturbation parameter, and the Hamiltonians H_0 and H_1 are assumed to be real analytic functions. The canonical Hamiltonian vector field generated by H_0 is completely integrable with the n independent integrals I_1, \dots, I_n . The phase space of this integrable system is foliated by n -dimensional invariant tori of the form $I = \text{const}$. Most of these tori typically carry quasiperiodic motions with n rationally independent frequencies, but there

¹ Division of Applied Mathematics, Brown University, Providence, Rhode Island 02912; e-mail: haller@cfm.brown.edu.

is also a set of tori with action value I' that satisfy resonance conditions of the form

$$\langle D_I H_0(I'), k \rangle = 0 \quad (2)$$

for some $k \in \mathbb{Z}^n$. These resonant tori form a dense *resonant set* in the phase space. In the generic case the KAM theory guarantees that most unperturbed tori outside a neighborhood of the resonant set survive for $\varepsilon > 0$. This implies that the perturbed Hamiltonian (1) is stable in the sense that most initial conditions remain confined to invariant tori for all times. This fact, however, does not prevent instability in a vicinity of the resonant set where the KAM tori are destroyed. In his classic paper Arnold⁽¹⁾ offered a model for this instability. His model system exhibits an $\mathcal{O}(1)$ variation in the action values for arbitrary small ε . The variation occurs along solutions that visit neighborhoods of lower dimensional hyperbolic or *whiskered* tori that form a transition chain.

It is well known, however, that some features of Arnold's example are nongeneric. Even more importantly, he introduced an additional small parameter to make the contributions from the nonresonant harmonics of the perturbation Hamiltonian H_1 as small as needed compared to the resonant harmonics. In reality, the amplitudes of nonresonant harmonics are very small, but not independent of the magnitude of the parameter ε , which multiplies the amplitudes of the resonant harmonics as well. This would normally result in exponentially small splittings of separatrices, a problem which is eliminated by Arnold's introduction of the second small parameter mentioned above. Nonetheless, it is widely believed that his construction does provide the fundamental mechanism for "*diffusion*" along single resonances in the phase space of the Hamiltonian (1). [By diffusion we mean $\mathcal{O}(1)$ displacement of initial conditions in the action space as $\varepsilon \rightarrow 0$, as described in ref. 2. See ref. 6 for a more precise definition.] Indeed, at least some of the nongeneric features of Arnold's example can be eliminated^(20,27,51) and the transition chains of tori can be constructed with full rigor for certain classes of problems.^(5,7)

To obtain a comprehensive picture of global diffusion along the resonant set, one also needs to understand the dynamics at the intersection of single resonances, where the resonance condition (2) is satisfied by two or more linearly independent integer vectors. Near such a multiple resonance the Hamiltonian can be reduced to an m -degree-of-freedom normal form, where $m \geq 2$ is the multiplicity of the resonance (see, e.g., refs. 8, 4, 2, 26, and 31). The corresponding normal form Hamiltonian can be viewed as that of m strongly coupled pendula, or, alternatively, the one describing the motion of a billiard ball in an external field on a periodic table. Clearly,

these problems are usually nonintegrable and defy any analytical approach. The exception is the case of $m = 2$, for which there are general variational results on the existence of periodic and asymptotically periodic solutions.^(11,3)

Recently, careful numerical experiments on symplectic maps suggested that Arnold diffusion near single resonances may be dominated by much faster motions in the action space that take place near multiple resonances.⁽²⁵⁾ Motivated by these observations, in ref. 17 we derived a normal form for the Hamiltonian (1) near the intersection of a stronger and a weaker resonance. Due to the decay of Fourier coefficients of analytic functions, the pendulum-type leading-order part of such a normal form turns out to be near-integrable. We showed the generic existence of a codimension-two *slow manifold* with motions that cross the weaker resonance along the stronger one at a speed of $\mathcal{O}(\sqrt{\varepsilon})$. Using Fenichel coordinates near the low manifold,^(10,21,30,22) we constructed an $\mathcal{O}(\sqrt{\varepsilon}^n)$ open neighborhood of the slow manifold which is also filled with similar crossing motions. This justifies the numerical observability of *cross-resonance diffusion* in weak-strong resonance “junctions.” (The measure of initial conditions involved in Arnold diffusion along a single resonance, as well as the average diffusion speed, appear to be exponentially small in $\sqrt{\varepsilon}$.) In conclusion, the results in ref. 17 establish the existence of a new, observable mechanism for “fast” diffusion across weak resonances.

At the same time, the results in ref. 17 naturally lead to some new questions regarding the nature of cross-resonance diffusion. First, does cross-resonance diffusion take place in the vicinity of trajectories that lie in the intersection of stable and unstable manifolds of invariant sets, as in the case of Arnold diffusion? If yes, is the corresponding chaotic behavior “stronger” than chaos near single resonances? Finally, can we find particular trajectories that appear to be good candidates for connecting regions with slow Arnold diffusion to others with fast cross-resonance diffusion?

In this paper, using “normally hyperbolic techniques,” we address the above questions. Our main result is the existence of generic families of motions that go through complicated transients before they cross the weaker resonance along the stronger one. These motions are nontrivial homoclinic or heteroclinic orbits asymptotic to sets that are close to lower dimensional invariant tori. The homoclinic orbits make repeated excursions before asymptoting to their limit sets. These excursions manifest themselves as repeated crossings of the surface corresponding to the strong resonance, as well as repeated pulses in the slowly varying resonant phase combination corresponding to the strong resonance. After these transients, the homoclinic orbits slowly cross the weaker resonance along the stronger resonance. We refer to this phenomenon as *multipulse homoclinic jumping* within the strong resonance. In a truncation of the normal form, these multipulse orbits lie in the intersection of stable and unstable manifolds to

tori which exhibit $\mathcal{O}(\sqrt{\varepsilon})$ splittings, i.e., at least one spitting angle between the manifolds is *not* exponentially small. As a result, the corresponding homoclinic chaos is much stronger than the one caused by exponentially small splittings in Arnold's diffusion near a single resonance. Finally, the multipulse orbits we construct continue to exist in a vicinity of the weaker resonance; thus they are good candidates for connections between Arnold's transition chain and the slow manifold at the center of the resonance junctions. We believe that further study of these orbits will shed light on how exactly the exponentially slow Arnold diffusion speeds up to velocities algebraic in $\sqrt{\varepsilon}$ near the intersection of two resonances.

We also study the bifurcations of the above multipulse orbits as the system parameters in the unperturbed Hamiltonian H_0 are varied. It turns out that the multipulse homoclinic orbits generically undergo a sequence of pulse-multiplying bifurcations. If one introduces an appropriate nonlinear scaling for the energies of the multipulse orbits and plots these scaled energies against the bifurcation parameter, the resulting bifurcation diagram turns out to be *universal*, i.e., independent of the given system and the given resonance. We call this bifurcation diagram the *homoclinic tree* (see Fig. 8). The intricate structure of this homoclinic tree indicates a high level of stochasticity close to the center of the resonance junction.

Based on these results, one generically expects an observable *multipulse intermittency* in diffusion at weak-strong resonance junctions. For fixed valued of the system parameters, this intermittency occurs when solutions diffusing along a single resonance (following Arnold's mechanism) reach an intersecting higher order resonance. As a result, the above-mentioned chaotic jumping within the strong resonance sets in and lasts on times scales $\mathcal{O}(1/\sqrt{\varepsilon})$. The measure of initial conditions affected by this intermittency is $\mathcal{O}(\sqrt{\varepsilon^n})$.

To illustrate that our results are applicable to concrete near-integrable systems, we explicitly verify the existence of multipulse intermittency for the three-degree-of-freedom mechanical model shown in Fig. 1. This system consists of three coaxial rigid bodies which are able to rotate about two fixed vertical shafts without any friction or damping. However, the rotation of the first body (on the top) is constrained by a torsional spring (for a detailed description of the model see Section 5). We chose this system for illustration for two reasons. First, it is a realistic example, since the Fourier expansion of the perturbed Hamiltonian is not a finite trigonometric polynomial. Second, we would like to highlight that such a simple mechanical system can already admit the type of complicated dynamics that we describe in this paper. We study our model system under the assumption that the eccentricities εr_1 and εr_2 of the two linear springs shown in Fig. 1 are small. We are interested in the behavior of the model near a family of

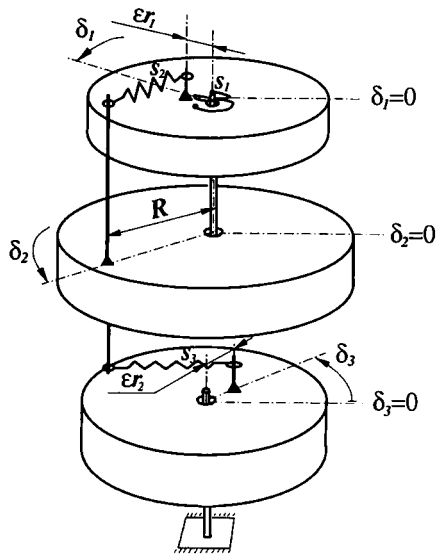


Fig. 1. The mechanical example.

resonance junctions. These junctions are characterized by a strong 1:1 resonance between the angular velocities of the second and the third body, and by a weaker 1:k₁ resonance between the torsional natural frequency of the first body and the angular velocity of the second body. We find that for sufficiently high values of k₁, there is an infinite number of resonance junctions in the phase space of the model which admit the universal, chaotic, multipulse intermittency that we described above.

The paper is organized as follows. In Section 2 we recall some results from ref. 17 on normal forms near weak-strong resonance junctions. In Section 3 we first describe an integrable limit of the truncation of this normal form, then proceed to establish the generic existence of multipulse intermittency in the truncated normal form. In Section 4 we extend our results to the full, n-degree-of-freedom normal form, which includes an exponentially small “tail.” In Section 5 we demonstrate our results on the mechanical model shown in Fig. 1. Finally, in Section 6 we summarize the main results and their implications.

2. NORMAL FORM FOR WEAK-STRONG DOUBLE RESONANCES

Throughout this paper we assume that for some fixed constant $\sigma > 0$ the complex extension $H_1(I, z; \varepsilon)$ of the Hamiltonian H_1 is analytic and

bounded in norm by a constant $K_\sigma > 0$ on the domain $|\text{Im } z_i| \leq \sigma$, $I \in S \subset \mathbb{R}^n$, for some bounded open set S . This implies that

$$H_1(I, \phi; \varepsilon) = \sum_{k \in \mathbb{Z}^n} h_k(I; \varepsilon) e^{i\langle k, \phi \rangle}, \quad \sup_{I \in S} \|H_1\| < K_\sigma$$

where $h_k \in \mathbb{C}$ denotes the Fourier coefficient of H_1 corresponding to the multiindex k . To measure the length of an integer vector $k = (k_1, \dots, k_n)$, we use the norm

$$|k| = \sum_{i=1}^n |k_i|$$

We shall study the unperturbed Hamiltonian H_0 near a point I' of the action space where precisely two independent resonance relationships of the form (2) are satisfied. This implies that the resonant module

$$M = \{k \in \mathbb{Z}^n \mid \langle D_I H_0(I'), k \rangle = 0\} \tag{3}$$

is two dimensional. Let $r_1 \in M$ be a minimal element of the module M , i.e., an integer vector with the property that for any $k \in M$, $|k| \geq |r_1|$ holds. Furthermore, let r_2 be an element of M which is linearly independent of r_1 and with modulus minimal among all elements of M that are linearly independent of r_1 . We require the resonance associated with r_2 to be higher in order than the one corresponding to r_1 and express this requirement by fixing $0 < \kappa < \sigma$ and picking positive constants $0 < \mu \ll c_0$ such that

$$\|h_{r_1}(I'; 0)\| > c_0, \quad |r_2| \geq L(\mu) = \text{Int} \left[\frac{2}{\kappa} \log \frac{C(n, K_\sigma, \kappa)}{\mu} \right] + 1 \tag{4}$$

where the constant $C > 0$ depends only on the parameters indicated. [The actual dependence of C on the parameters is $C(n, K_\sigma, \kappa) = 4^{n+1} e^{1-n} \kappa^{-n} (n-1)^{n-1} K_\sigma$.]

In a vicinity of the double resonance we introduce the new coordinates $(A, \alpha) \in \mathbb{R}^2 \times \mathbb{T}^2$ and $(B, \beta) \in \mathbb{R}^{n-2} \times \mathbb{T}^{n-2}$ by letting

$$\sqrt{\varepsilon} \begin{pmatrix} A \\ B \end{pmatrix} = (T')^{-1} (I - I'), \quad \begin{pmatrix} \alpha \\ \beta \end{pmatrix} = T\phi$$

where the integer matrix $T \in \mathbb{R}^{n \times n}$ with $|\det T| = 1$ contains r_1 and r_2 in its first two rows, respectively, and the rest of its rows are linearly independent of the first two. As described in ref. 2, repeated averaging with respect to

the “fast” angles β and the additional scaling $\beta \rightarrow \sqrt{\varepsilon} B$ brings the Hamiltonian H to the normal form

$$H(A, \alpha, B, \beta; \varepsilon) = \sqrt{\varepsilon} \langle b, B \rangle + \sqrt{\varepsilon} [H_{\text{pend}}(A, \alpha) + \sqrt{\varepsilon} H_2(A, \alpha, B; \sqrt{\varepsilon})] + e^{-c/\varepsilon^\nu} H_3(A, \alpha, B, \beta; \sqrt{\varepsilon}) \tag{5}$$

with $c > 0$ and $\nu = 1/8n(n + 1)$. (For brevity we do not describe the precise domain of definition of this Hamiltonian, as it is not used in our analysis, but see ref. 4 for details.) In (5), $b \in \mathbb{R}^{n-2}$ contains the last $n - 2$ elements of the vector $TD_j H_0(I')$, the functions H_2 and H_3 are analytic in their arguments, and the pendulum-type Hamiltonian H_{pend} is of the form

$$H_{\text{pend}}(A, \alpha) = \frac{1}{2} \langle A, P(\mu) A \rangle + V_1(\alpha_1; \mu) + \mu V_2(\alpha; \mu) \tag{6}$$

with

$$V_1(\alpha_1; \mu) = \sum_{p_1=0}^{L(\mu)/|r_1|} \tilde{h}_{(p_1, 0)} e^{ip_1 \alpha_1}$$

$$V_2(\alpha; \mu) = \sum_{|p_1 r_1 + p_2 r_2| > L(\mu)} \frac{\tilde{h}_p}{\mu} e^{i \langle p, \alpha \rangle}, \quad 0 < \mu \ll c_0 \tag{7}$$

The symmetric matrix $P \in \mathbb{R}^{2 \times 2}$ appearing in (6) is the first 2×2 minor of the matrix $TD_j^2 H_0(I') T'$; hence on a compact set of I' values and for fixed $r_1 \in M$, its norm obeys the estimate

$$\|P(\mu)\| < K_1 |r_2|^2 < K_2 \left(\log \frac{1}{\mu} \right)^2 \tag{8}$$

for appropriate positive constants K_j . The Fourier coefficients in the “potentials” V_1 and V_2 are defined as

$$\tilde{h}_p = h_k(I'; 0), \quad k = p_1 r_1 + p_2 r_2 \tag{9}$$

Furthermore, both V_1 and V_2 and their derivatives admit μ -independent bounds, in particular,

$$|V_1| < K_\sigma, \quad |V_2| < 1, \quad \|D_\phi^k V_2\| \leq |k|! \kappa^{-|k|} \tag{10}$$

As usual, to obtain the normal form (5), one has to assume that the $n - 2$ frequencies corresponding to the fast angles β satisfy appropriate Diophantine conditions.⁽⁴⁾ We finally note that the normal form Hamiltonian (5)

generates the corresponding Hamiltonian vector field through the symplectic form

$$\omega = d\alpha \wedge dA + \sqrt{\varepsilon} d\beta \wedge dB \quad (11)$$

As we shall see, one may treat the Hamiltonian (6) as close to integrable, even though, strictly speaking, the formal limit $\mu = 0$ is not well defined. The reason is that $\mu = 0$ would mean an “infinitely high order” resonance by Eq. (4), and hence no Fourier term would satisfy the summation condition in the definition of the potential V_2 . Also note that the (A, α) components of the Hamiltonian vector field deriving from (5) decouple from the system up to exponentially high orders.

We would like to study the pendulum Hamiltonian (6) as a perturbation of the integrable Hamiltonian

$$H_{\text{pend}}^0(A, \alpha) = \frac{1}{2} \langle A, P(\mu) A \rangle + V_1(\alpha_1; \mu) \quad (12)$$

where we pointed out the dependence of the matrix P and the potential V_2 on the parameter $\mu > 0$. To this end, we select and fix a concrete strong resonance corresponding to the generator $r_1 \in M$ and pick an action value I'_0 on the resonant hypersurface $\langle D_I H_0(I), r_1 \rangle = 0$. We also consider a fixed, open ball $\mathcal{B} \subset \mathbb{R}^n$ in the action space which is centered around $I = I'_0$. As a nondegeneracy condition on the Hamiltonian H_{pend}^0 , we assume that there exists a constant $c_1 > 0$ and for all $I' \in \mathcal{B}$ and $0 < \mu < \mu_0$ there exists an angle $\alpha_{10}(\mu)$ such that

$$D_{x_1} V_1(\alpha_{10}; \mu) = 0, \quad p_{11}(\mu) D_{x_1}^2 V_1(\alpha_{10}; \mu) > c_1 > 0 \quad (13)$$

Remark 2.1. It is important to note that a μ -independent constant c_1 with the above properties can be found for $\mu > 0$ sufficiently small, because for fixed I' , $|p_{11}|$ is a *nondecreasing* function of μ as $\mu \rightarrow 0$. If p_{11} and V_1 have no explicit μ dependence in a given application, then the constant c_1 exists globally in the action space, hence the restriction of the resonant action values I' to the bounded ball \mathcal{B} is not necessary. This is the case, e.g., in our example in Section 5.

It is easy to verify that for any fixed A_2 value, the above nondegeneracy conditions imply the existence of a saddle point $\alpha_1 = \alpha_{10}$, $A_1 = -p_{12} A_2 / p_{11}$ for the (α_1, A_1) component of the equations generated by the Hamiltonian H_{pend}^0 (see the next section). Furthermore, the modulus of the corresponding real eigenvalues is bounded away from zero by the constant c_1 . For later purpose we also require the nondegeneracy condition

$$\det P \neq 0 \quad (14)$$

In the following we first analyze the two-degree-of-freedom, near-integrable pendulum Hamiltonian H_{pend} which decouples from the full normalized Hamiltonian if we neglect the exponentially small tail of the normal form. Then in Section 4 we extend our results to the full Hamiltonian (5).

3. DYNAMICS OF THE PENDULUM HAMILTONIAN

In this section we study a slightly modified version of H_{pend} of the form

$$H_{\text{pend}}(A, \alpha; \rho) = \frac{1}{2} \langle A, PA \rangle + V_1(\alpha_1; \mu) + \rho V_2(\alpha; \mu) \tag{15}$$

with the auxiliary parameter $0 \leq \rho \leq \mu$. We will first fix μ and establish results for sufficiently small values of ρ . As a second step, we will show that these results continue to hold for $\rho = \mu$ provided the fixed μ is small enough.

3.1. The Integrable Limit $\rho = 0$

The Hamiltonian vector field corresponding to $H_{\text{pend}}(A, \alpha; 0)$ [defined in (15)] takes the form

$$\begin{aligned} \dot{\alpha}_1 &= p_{11}A_1 + p_{12}A_2 \\ \dot{A}_1 &= -D_{\alpha_1}V_1(\alpha_1; \mu) \\ \dot{\alpha}_2 &= p_{12}A_1 + p_{22}A_2 \\ \dot{A}_2 &= 0 \end{aligned} \tag{16}$$

which shows that A_2 is an integral for this system. We recall that the parameter μ is arbitrarily small but fixed, and the constants p_{ij} depend on μ . Generically, the periodic potential V_1 has isolated local minima and at least one of these extrema, α_{10} , will satisfy the nondegeneracy condition (13). We can directly see from Eq. (16) that any such local extremum α_{10} gives rise to a two-dimensional invariant manifold for (16) of the form

$$\mathcal{M}_0 = \left\{ (A, \alpha) \mid \alpha_1 = \alpha_{10}, A_1 = -\frac{p_{12}}{p_{11}} A_2 \right\} \tag{17}$$

Moreover, this manifold is of ‘‘saddle type,’’ i.e., normally hyperbolic.^(9,32) In this paper we are interested in structures near multiple resonances that influence large sets of initial conditions, which is why we focus on normally

hyperbolic manifolds with their attendant stable and unstable manifolds. The most important hyperbolic manifolds of the form \mathcal{M}_0 are those whose stable and unstable manifolds serve as *boundaries for the stronger resonance*. A boundary for the strong resonance is a hypersurface that separates solutions of (1) that cross the stronger resonance from those that do not. We now make the following assumption:

(A1) $|V_1(\alpha_1; \mu)| < |V_1(\alpha_{10}; \mu)|$, i.e., α_{10} is a unique global extremum point for the potential V_1 .

Note that by the periodicity and nondegeneracy of V_1 , it certainly possesses isolated global minima and maxima. The above assumption covers the generic case when the extrema are unique. In such a case the boundary of the strong resonance has precisely two components, W^+ and W^- , which form a symmetric pair of manifolds homoclinic to \mathcal{M}_0 . In Fig. 2 we show the geometry of these homoclinic manifolds by factoring out the angular coordinate α_2 . We also indicate two important three-dimensional surfaces in the figure that appear as planes. The plane $A_1 = 0$ corresponds to the resonance hypersurface associated with the stronger r_1 resonance, while $A_2 = 0$ describes the hypersurface of the weaker r_2 resonance. We call these hypersurfaces the *cores of the respective resonances*.

All solutions in \mathcal{M}_0 with $A_2 \neq 0$ are periodic and correspond to the limits of $(n-1)$ -dimensional whiskered tori of the full normal form Hamiltonian. It is not hard to see that in a neighborhood of \mathcal{M}_0 the energy surfaces containing the periodic orbits act as barriers that prevent solutions from crossing the core of the weak resonance along the strong resonance. However, for $\rho > 0$, these barriers are typically destroyed by the perturbation in the vicinity of the weak resonance. The reason is that for $\rho = 0$ a

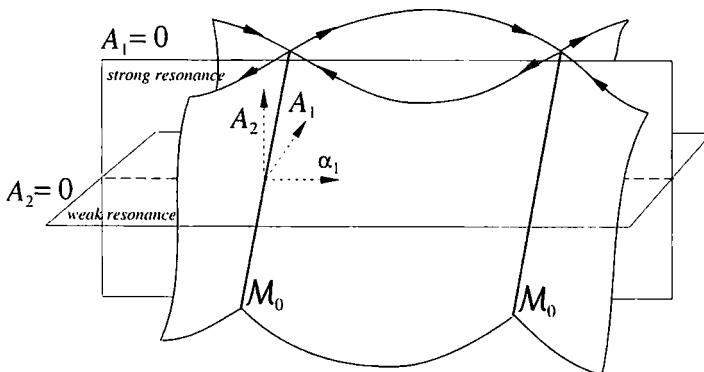


Fig. 2. The manifold \mathcal{M}_0 and its stable and unstable manifolds.

singularity occurs in \mathcal{M}_0 at $A_2=0$: the periodic orbits degenerate into a circle of equilibria \mathcal{E}_0 .

Any fixed point in \mathcal{E}_0 is connected to another fixed point in \mathcal{E}_0 by a pair of heteroclinic orbits. We call the change of the slow angle α_2 on these connections the *phase shift*, and denote it by $\Delta\alpha_2^\pm$ for heteroclinic orbits in the homoclinic manifold W^\pm . From (16) we obtain that

$$\Delta\alpha_2^+ = \int_{-\infty}^{+\infty} p_{12} A_1^+(t) dt = \frac{p_{12}}{p_{11}} \int_{-\infty}^{+\infty} \dot{\alpha}_1^+(t) dt = \frac{2\pi p_{12}}{p_{11}}, \quad \Delta\alpha_2^- = -\Delta\alpha_2^+ \quad (18)$$

where $(A_1^+(t), \alpha_1^+(t))$ is the heteroclinic solution that lies in W^+ and connects fixed points in \mathcal{E}_0 .

The circle \mathcal{E}_0 is of central importance in our study, as it corresponds to an invariant $(n-1)$ -dimensional torus of the integrable Hamiltonian H_0 . This torus is located precisely at the center of the resonance junction, i.e., at the intersection of the cores of the weak and the strong resonances. In the limit $\rho=0$ of the normal form, the torus is foliated by one-parameter families of $(n-2)$ -dimensional invariant tori which appear in system (16) as the equilibria in \mathcal{E}_0 .

3.2. The Perturbed Pendulum Hamiltonian with $\rho > 0$

We now turn to the study of the Hamiltonian H_{pend} with $\rho > 0$, which generates the Hamiltonian vector field

$$\begin{aligned} \dot{\alpha}_1 &= p_{11} A_1 + p_{12} A_2 \\ \dot{A}_1 &= -D_{\alpha_1} V_1(\alpha_1; \mu) - \rho D_{\alpha_1} V_2(\alpha_1, \alpha_2; \mu) \\ \dot{\alpha}_2 &= p_{12} A_1 + p_{22} A_2 \\ \dot{A}_2 &= -\rho D_{\alpha_2} V_1(\alpha_1, \alpha_2; \mu) \end{aligned} \quad (19)$$

Well-known invariant manifold results guarantee that the manifold \mathcal{M}_0 smoothly perturbs into an $\mathcal{O}(\rho)$ C^r -close invariant manifold \mathcal{M}_ρ for any finite integer $r \geq 1$ (see, e.g., ref. 9). Furthermore, it is shown in ref. 14 that manifolds of the form \mathcal{M}_ρ carry a one-degree-of-freedom Hamiltonian dynamics that slightly deforms but preserves the periodic solutions on \mathcal{M}_ρ which are sufficiently separated from the $A_2=0$ core of the weak resonance. Using the area-preserving nature of appropriate Poincaré maps, one can easily conclude that the stable and unstable manifolds of the surviving periodic orbits still intersect (see, e.g., ref. 33 for an argument). In the generic case the stable and unstable manifolds will intersect transversely, giving rise to isolated transverse homoclinic orbits and nearby

invariant Cantor sets with chaotic dynamics. To verify transversality in given examples, one can use the Melnikov function

$$M(\alpha_{20}, A_2) = \int_{-\infty}^{\infty} \left. \{H_{\text{pend}}^0, V_2\} \right|_{x^h(t)} dt \tag{20}$$

as derived, e.g., in ref. 19 for two-degree-of-freedom Hamiltonian systems of the form (19). Here $x^h(t) = (A(t), \alpha(t))$ denotes an unperturbed homoclinic solution with $(A_1(t), A_2, \alpha_1(t), \alpha_{20} + \omega_0 t)$, which is homoclinic to a periodic solution in \mathcal{M}_0 . The frequency of the periodic solution is easily computed to be $\omega_0 = A_2 \det P/p_{11}$. Hence for periodic orbits with $A_2 = \mathcal{O}(\sqrt{\rho})$, one can perform the Melnikov calculation and then take the limit $\rho \rightarrow \mu$. The result will be conclusive, since the frequency vector remains bounded and nonzero for small $\mu > 0$ by the estimate (8) and the nondegeneracy conditions (13) and (14). For periodic orbits with $\mathcal{O}(1)$ values of A_2 , the Melnikov integral will depend on the frequency $\omega_0 = \mathcal{O}((\log 1/\mu)^2)$, which becomes “fast” when one finally takes the limit $\rho \rightarrow \mu$ for some small value of μ . Hence a formal Melnikov calculation becomes inconclusive, as it yields exponentially small splittings. It appears, however, that appropriate extensions of the results in ref. 12 could be applied to verify transversality in this case.

3.2.1. The Slow Manifold. Note that all solutions described above remain outside a neighborhood of the core of the weak resonance ($A_2 = 0$). In order to understand the dynamics near the weaker resonance, we shall concentrate on energy surfaces that intersect an $\mathcal{O}(\sqrt{\rho})$ neighborhood of the plane $A_2 = 0$. In such a neighborhood the above statements about the perturbed dynamics are not valid since the periodic orbits on \mathcal{M}_ρ are not guaranteed to survive.

First, to understand what happens on \mathcal{M}_ρ close to the weak resonance, we introduce the usual resonance scaling

$$A_2 = \sqrt{\rho} \eta$$

which “blows up” a neighborhood of the core of the weak resonance. (In the context of resonant circles on invariant manifolds, this scaling was apparently used first in ref. 24.) Then it is easy to verify that the Hamiltonian flow on \mathcal{M}_ρ near $A_2 = 0$ is generated by the equations

$$\begin{aligned} \dot{\alpha}_2 &= \sqrt{\rho} D_\eta \mathcal{H}(\eta, \alpha_2) + \mathcal{O}(\rho^{3/2}) \\ \dot{\eta} &= -\sqrt{\rho} D_{\alpha_2} \mathcal{H}(\eta, \alpha_2) + \mathcal{O}(\rho^{3/2}) \end{aligned} \tag{21}$$

which are, in general, only canonical at leading order. After a rescaling of time by $\sqrt{\rho}$, the leading-order terms in (21) derive from the *reduced Hamiltonian* \mathcal{H} given by

$$\mathcal{H}(\eta, \alpha_2) = \frac{1}{2} \frac{\det P}{\rho_{11}} \eta^2 + V_2(\alpha_{10}, \alpha_2; \mu) \tag{22}$$

as seen from the general results in ref. 14 for perturbed circles of equilibria in Hamiltonian systems. Nonsingular level curves of \mathcal{H} smoothly approximate actual trajectories of the restricted vector field (21) with $\mathcal{O}(\sqrt{\rho})$ precision [which means $\mathcal{O}(\rho)$ precision in the original (A_2, α_2) coordinates]. The equations in (21) also show that \mathcal{M}_ρ is locally a *slow manifold* near $A_2 = 0$ with a characteristic time scale $\mathcal{O}(1/\sqrt{\rho})$. By the non-degeneracy condition (14), all slow motions enclosed by the separatrices of the reduced Hamiltonian \mathcal{H} cross the core of the weak resonance and connect points that are $\mathcal{O}(\sqrt{\rho})$ apart in their A_2 coordinates. In ref. 17 we used slow manifolds of the form \mathcal{M}_ρ to construct an open set of initial conditions for which solutions cross the weak resonance along the strong resonance.

3.2.2. Multipulse Homoclinics. Our main goal is to establish the existence of solutions that are doubly asymptotic to slow solutions on \mathcal{M}_ρ , but exhibit fast excursions from the slow manifold on intermediate time scales. The significance of such homoclinic or heteroclinic solutions is that they describe motions that pass through the weak resonance along the strong one after exhibiting fast transients. Since all slow motions degenerate into sets of equilibria at the limit $\rho = 0$, regular perturbation methods cannot be used to construct orbits asymptotic to them for $\rho > 0$. In particular, the basic assumptions of the usual Melnikov method for the study of two-degree-of-freedom near-integrable Hamiltonian systems (see, e.g., ref. 19) are not satisfied. Instead, we shall use the *energy-phase method*,^(15,16) which has been developed precisely for detecting motions doubly asymptotic to hyperbolic slow manifolds.

First, for any integer $N \geq 1$ we define the N th-order energy-difference function $\Delta^N \mathcal{H}(\alpha_2)$ as

$$\Delta^N \mathcal{H}(\alpha_2) = V_2(\alpha_{10}, \alpha_2 + N\Delta\alpha_2^+; \mu) - V_2(\alpha_{10}, \alpha_2; \mu) \tag{23}$$

As one can verify from (22), $\rho\Delta^N \mathcal{H}(\alpha_2)$ measures the leading-order energy difference between two points on the slow manifold that were originally connected by a chain of N heteroclinic orbits lying in W^+ . We shall be concerned with the existence of two basic types of orbits that are asymptotic to slow solutions on \mathcal{M}_ρ . In the following definitions *segments*

refer to compact, connected subsets of orbits. We also recall that by the *core* of the strong resonance we mean the surface $\eta = 0$.

Definition 3.1. An orbit homoclinic to the manifold \mathcal{M}_ρ is an *N-pulse librational orbit* if it has N segments $\mathcal{O}(\sqrt{\rho})$ C^1 -close to unperturbed heteroclinic connections and it intersects the core of the strong resonance outside a fixed [i.e., $\mathcal{O}(1)$ as $\rho \rightarrow 0$] neighborhood of \mathcal{M}_ρ (see Fig. 3a) $N - 2$ times.

Definition 3.2. An orbit homoclinic to the manifold \mathcal{M}_ρ is an *N-pulse rotational orbit* if it has N segments $\mathcal{O}(\sqrt{\rho})$ C^1 -close to unperturbed heteroclinic connections and it does *not* intersect the core of the strong resonance outside a fixed neighborhood of \mathcal{M}_ρ (see Fig. 3b).

Definition 3.3. An orbit homoclinic to the manifold \mathcal{M}_ρ is an *N-pulse passing orbit* if it has N segments $\mathcal{O}(\sqrt{\rho})$ C^1 -close to unperturbed heteroclinic connections and it intersects the core of the strong resonance precisely once outside a fixed neighborhood of \mathcal{M}_ρ (see Fig. 3c).

Clearly, the librational, rotational, and passing orbits are either homoclinic or heteroclinic to slow solutions on \mathcal{M}_ρ . We finally introduce a definition that will be used to describe the order of transversality of stable and unstable manifolds along multipulse homoclinic orbits.

Definition 3.4. Let X and Y be two smooth, n -dimensional manifolds embedded in \mathbb{R}^{2n} that intersect at a point $p \in \mathbb{R}^{2n}$. Let $T_p X$ denote the

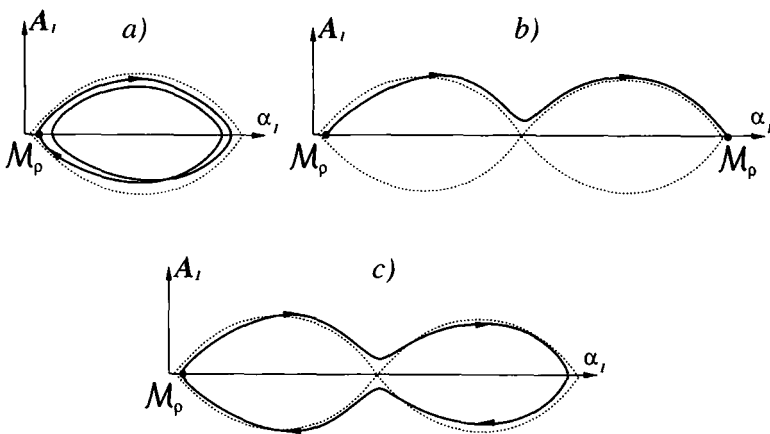


Fig. 3. Projections of (a) librational homoclinic orbits with $N = 4$, (b) rotational homoclinic orbits with $N = 2$, and (c) passing homoclinic orbits with $N = 4$ onto the (α_1, A_1) plane.

tangent space to X at p , and let $N_p Y$ denote the normal space to Y at p . Then we define the *maximal splitting angle* of X and Y at the point p as

$$a(p) = \max_{u,v} \{ \langle u, v \rangle \mid u \in T_p X, v \in N_p Y, |u| = |v| = 1 \}$$

Note that this definition is obviously symmetric in X and Y . Furthermore, if we pick two orthonormal bases $\{u_i\}_{i=1}^n \subset T_p X$ and $\{v_j\}_{j=1}^n \subset N_p Y$ and define the *splitting matrix*

$$M_p = \{ \langle u_i, v_j \rangle \}_{i,j \in \mathbb{R}^{n \times n}} \tag{24}$$

then we have

$$a(p) = \|M_p\| \tag{25}$$

This shows that although the entries and the eigenvalues of M_p generally depend on the choice of the bases, the norm of M_p is invariant and can be thought of as the sine of the maximal angle enclosed by the two manifolds at the point p . The entries of M_p characterize the order of magnitude of the angles between two basis vectors from $T_p X$ and $N_p Y$.

We can now prove the following main result on the existence of multi-pulse homoclinic orbits.

Theorem 3.1. Suppose that assumption (A1) is satisfied and γ is a periodic orbit of the reduced Hamiltonian \mathcal{H} . Then for $\rho > 0$ small enough the following hold.

(i) If $p_{11} \Delta^1 \mathcal{H} \mid \gamma < 0$, then the system (19) admits a continuous family of slow periodic solutions close to γ , each with at least four two-pulse, librational homoclinic orbits.

(ii) If $p_{11} \Delta^k \mathcal{H} \mid \gamma > 0$ for $k = 1, \dots, N - 1$ and $p_{11} \Delta^N \mathcal{H} \mid \gamma < 0$, then the system (19) admits a continuous family of slow periodic solutions close to γ , each with at least four $2N$ -pulse, passing homoclinic orbits. Furthermore, there are no lower pulse orbits homoclinic to orbits in the family.

(iii) If $p_{11} \Delta^k \mathcal{H} \mid \gamma > 0$ for $k = 1, \dots, N - 1$ and $\Delta^N \mathcal{H}$ has m transverse zeros on γ , then the system (19) admits a continuous family of slow periodic solutions close to γ , each with at least $4m$ transverse, N -pulse rotational heteroclinic orbits backward asymptotic to it. The heteroclinic orbits are forward asymptotic to slow orbits of (21) that pass near points of the form $(\eta_N, \alpha_{2N} + \Delta \alpha_2^+)$, where (η_N, α_{2N}) is a transverse zero of $\Delta^N \mathcal{H}$ on γ . Again, there are no lower pulse orbits backward asymptotic to members of this family.

(iv) The maximal splitting angle along the rotational heteroclinic orbits in statement (iii) is $\mathcal{O}(\sqrt{\rho})$ as $\rho \rightarrow 0$.

Proof. The proof follows the ideas described in refs. 15 and 16, so we only outline the main steps. Since \mathcal{H} generates the leading-order terms of the Hamiltonian vector field on the slow manifold, there exists a family of slow periodic orbits on \mathcal{M}_ρ whose projections on the (η, α_2) plane are $\mathcal{O}(\sqrt{\rho})$ C^1 -close to γ . We pick a periodic orbit γ_ρ^- from this family and follow one of the two components of its two-dimensional unstable manifold $W^u(\gamma_\rho^-)$. This manifold leaves a neighborhood of \mathcal{M}_ρ , stays close to W^+ , and enters a neighborhood of \mathcal{M}_ρ again by intersecting a two-dimensional Poincaré section Σ^+ which is transversal to the flow within the energy surface containing γ_ρ^- (see Fig. 4a). The intersection is a smooth curve \mathcal{D}_1 which has the property that its (η, ϕ) projection is C^1 -close to $\gamma + \Delta\alpha_2^+$ (i.e., to the image of the orbit γ under a shift by the angle $\Delta\alpha_2^+$).

Suppose that γ_ρ^+ is another slow orbit of the restricted system (21) with the same energy as γ_ρ^- . Then the local stable manifold $W_{\text{loc}}^s(\gamma_\rho^+)$ also intersects the section Σ^+ in a curve \mathcal{E}_1 with (η, ϕ) projection C^1 -close to γ_ρ^+ . By the implicit function theorem, $W^u(\gamma_\rho^-)$ intersects $W^s(\gamma_\rho^+)$ transversely if $\gamma + \Delta\alpha_2^+$ intersects some other isoenergetic level curve of the reduced Hamiltonian \mathcal{H} . But this is equivalent to the condition that $\Delta^1\mathcal{H}$ has a transverse zero on γ , which proves (iii) for $N = 1$. If, however, $\Delta^1\mathcal{H}$ has no zero on γ then the unstable manifold $W^u(\gamma_\rho^-)$ leaves a neighborhood of \mathcal{M}_ρ without intersecting the stable manifold of a slow orbit and travels in a neighborhood of either W^+ or W^- . This can be decided by comparing the energy of $W^u(\gamma_\rho^-)$ to energies of nearby solutions in the three-dimensional stable manifold $W_{\text{loc}}^s(\mathcal{M}_\rho)$. At leading order, the difference in energies is just given by the function $\Delta^1\mathcal{H} | \gamma$ (see [16] for details). Consequently, if $\Delta^1\mathcal{H} | \gamma > 0$ (or $\Delta^1\mathcal{H} | \gamma < 0$) then $W^u(\gamma_\rho^-)$ passes by $W_{\text{loc}}^s(\mathcal{M}_\rho)$ in the direction of (or in the direction opposite to) the gradient DH_{pend} on Σ^+ . Computing the gradient DH_{pend} we immediately see that $p_{11}\Delta^1\mathcal{H} | \gamma > 0$ implies

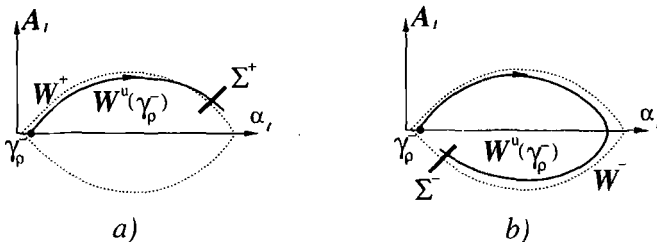


Fig. 4. The Poincaré sections Σ^+ and Σ^- .

a passage in the direction of W^+ and $p_{11} \Delta^1 \mathcal{H} \mid \gamma < 0$ implies a crossing of the strong resonance $A_1 = 0$ in the direction of W^- . In this latter case, by standard Gronwall estimates, the unstable manifold $W^u(\gamma_\rho^-)$ returns to a neighborhood of the slow manifold and intersects a two-dimensional Poincaré section Σ^- (see Fig. 4b). This time the intersection curve $\mathcal{D}_2 = \Sigma^- \cap W^u(\gamma_\rho^-)$ has an (η, α_2) -projection which is C^1 -close to $\gamma + \Delta\alpha_2^+ + \Delta\alpha_2^- \equiv \gamma$. At the same time, the curve $\mathcal{E}_2 = \Sigma^- \cap W_{loc}^s(\gamma_\rho^+)$ also projects to a curve that is C^1 -close to γ . Since Σ^- is a graph over the variables η and α_2 and \mathcal{D}_2 and \mathcal{E}_2 are closed curves of the same area, we obtain that $W^u(\gamma_\rho^-)$ and $W_{loc}^s(\gamma_\rho^+)$ must intersect in at least two librational, 2-pulse homoclinic orbits. Repeating the same argument for the other component of $W^u(\gamma_\rho^-)$ proves statement (i) of the theorem.

It remains to consider the case of $p_{11} \Delta^1 \mathcal{H} \mid \gamma > 0$ which implies that the unstable manifold of γ_ρ^- passes in the direction of W^+ . Then $W^u(\gamma_\rho^-)$ passes in a neighborhood of W^+ and reintersects the Poincaré section Σ^+ . Repeating the same reasoning as above, we obtain that if $\Delta^2 \mathcal{H} \mid \gamma$ has a transverse zero then there exists a slow orbit γ_ρ^+ such that $W^u(\gamma_\rho^-)$ intersects $W_{loc}^s(\gamma_\rho^+)$ transversely upon its second intersection with Σ^+ . This proves statement (iii) for $N=2$. If, however, $\Delta^2 \mathcal{H} \mid \gamma$ has no zero, then $W^u(\gamma_\rho^-)$ again passes near \mathcal{M}_ρ either in the direction of W^+ or of W^- . The passage direction is again determined by the sign of the function $p_{11} \Delta^1 \mathcal{H} \mid \gamma$. If this sign is negative then $W^u(\gamma_\rho^-)$ crosses the strong resonance and returns to the section Σ^- . The fact that $p_{11} \Delta^1 \mathcal{H} \mid \gamma > 0$ ensures that $W^u(\gamma_\rho^-)$ again passes \mathcal{M}_ρ in the direction of W^- and its subsequent intersection with Σ^- has an (η, α_2) -projection that is C^1 -close to γ_ρ^- . This proves statement (ii) for $N=2$. Then statements (ii) and (iii) follow for arbitrary N by induction. (The number of the homoclinic or heteroclinic orbits in these statements follows from the fact that our entire construction can be repeated for the other connected component of the unstable manifold $W^u(\gamma_\rho^-)$.)

Finally, let an N -pulse rotational multi-pulse orbit described in statement (iii) lie in the intersection $W^u(\gamma_\rho^-) \cap W^s(\gamma_\rho^+)$. Consider the intersection curves $\mathcal{D}_N = W^u(\gamma_\rho^-) \cap \Sigma^+$ and $\mathcal{E}_N = W^s(\gamma_\rho^+) \cap \Sigma^+$ with the Poincaré section Σ^+ . As we noted above, these intersections are graphs over the (η, α_2) variables and are $\mathcal{O}(\sqrt{\rho})$ C^1 -close to the curves $\gamma_\rho^- + N\Delta\alpha_2^+$ and γ_ρ^+ , respectively. Hence, if \mathcal{E}_N and \mathcal{D}_N intersect transversally, then the intersection angle is $\mathcal{O}(1)$ in terms of the (η, α_2) coordinates as $\rho \rightarrow 0$ (see Fig. 5). In terms of the (A_2, α_2) coordinates, this means an $\mathcal{O}(\sqrt{\rho})$ angle. Since the stable and unstable manifolds are two dimensional and their intersection is one dimensional, computing the intersection matrix M_ρ for $p \in \mathcal{D}_N \cap \mathcal{E}_N$ in an appropriate basis immediately yields the maximal splitting angle $a(p) = \|M_\rho\| = \mathcal{O}(\sqrt{\rho})$. This proves statement (iv). ■

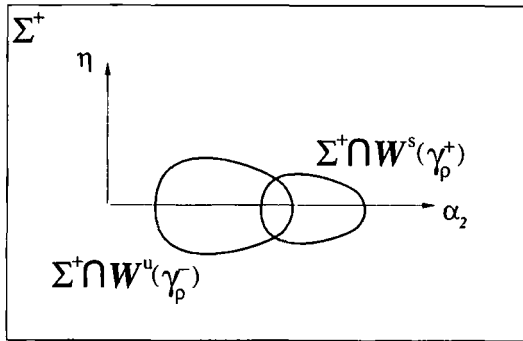


Fig. 5. Intersections of the stable and unstable manifolds of the periodic solutions γ_p^\pm with the Poincaré section Σ^+ .

Remark 3.1. If no other level curve of \mathcal{H} has the same energy as γ , then the librational orbits guaranteed by statement (i) of the theorem are necessarily asymptotic to the same slow periodic orbit in forward time as well, i.e., they are homoclinic orbits.

Remark 3.2. The “large” splitting angles described in statement (iii) of the above theorem are due to the singular perturbation nature of our system: the stable and unstable manifolds of slow periodic solutions are not smooth continuations of unperturbed structures. Rather, they are created by the $\mathcal{O}(\rho)$ perturbation in the breakup of the circle of equilibria on \mathcal{M}_0 .

3.2.3. Universal Bifurcations: The Homoclinic Tree. We now apply Theorem 3.1 to periodic solutions with the property described in Remark 3.1. In particular we assume that:

- (A2) There exists a connected open set \mathcal{D}_0 that contains an elliptic fixed point of \mathcal{H} and is entirely filled with periodic orbits which are energetically unique (i.e., each is the only connected component of a level set of \mathcal{H}).

In the generic case the global minima and maxima of the potential part $V_2(\alpha_{10}, \alpha_2; \mu)$ of \mathcal{H} are energetically unique; hence there exists an elliptic equilibrium for the reduced Hamiltonian \mathcal{H} with an open neighborhood which is filled with orbits satisfying assumption (A2). We select the maximal such connected neighborhood and denote in by \mathcal{D}_0 . Note that \mathcal{D}_0 is always bounded by a homoclinic orbit or by a pair of heteroclinic orbits. In Fig. 6a we show the construction of \mathcal{D}_0 in a homoclinic case when $\det P/p_{11} < 0$, which mans that the kinetic energy-type term in the reduced Hamiltonian \mathcal{H} has a positive “mass.” We denote the angular diameter of

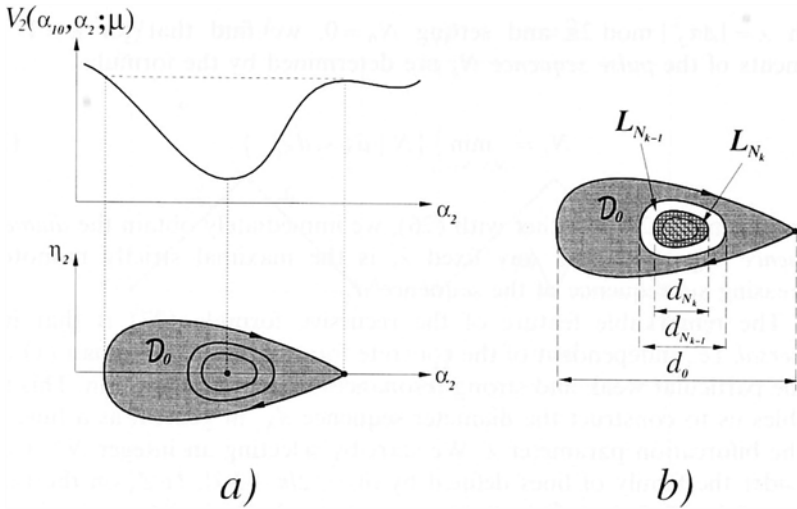


Fig. 6. The domain \mathcal{D}_0 and the layers L_{N_k} .

\mathcal{D}_0 by d_0 . We want to find conditions under which there are multipulse orbits backward asymptotic to slow orbits close to those of \mathcal{H} in \mathcal{D}_0 . By Remark 3.1 and Assumption (A2), these multipulse orbits are necessarily homoclinic to slow solutions.

We now proceed by interpreting the assumptions of Theorem 3.1 in geometric terms for the case covered by statement (iii). We observe that the condition $\Delta^k \mathcal{H} | \gamma \neq 0$ for $k = 1, \dots, N - 1$ means the following: Shifting the level curve γ of the reduced Hamiltonian \mathcal{H} $N - 1$ times by the amount of the phase shift $\Delta\alpha_2^+$ in the α_2 direction, we always find that the shifted curve does not intersect any other level curve of \mathcal{H} with the same energy. For any $\gamma \in \mathcal{D}_0$ this observation implies that the minimal index k for which $\Delta^k \mathcal{H} | \gamma$ has a zero is the minimal number of shifts by $\Delta\alpha_2^+$ such that $\gamma + \Delta\alpha_2^+$ has an intersection with γ . This number is well defined for any closed orbit $\gamma \in \mathcal{D}_0$ and we call it the *pulse number* of γ [denoted $N(\gamma)$].

It is easy to see that for fixed $\Delta\alpha_2^+$, \mathcal{D}_0 can be divided into “layers” of orbits with different pulse numbers. The number of layers is infinite if $2\pi/\Delta\alpha_2^+$ is an irrational number and is finite otherwise. If N_1, N_2, \dots is the sequence of pulse numbers associated with the layers L_{N_1}, L_{N_2}, \dots (see Fig. 6b), then the inner boundary of the layer L_{N_k} is a periodic orbit γ_{N_k} such that $N = N_k$ is the minimal positive integer for which $\gamma_{N_k} + N\Delta\alpha_2^+$ becomes tangent to γ_{N_k} . Therefore, introducing the sequence

$$d_N = \min_{l \in \mathbb{Z}} |2l\pi - N\lambda|, \quad N \geq 1 \tag{26}$$

with $\lambda = |\Delta\alpha_2^+| \bmod 2\pi$ and setting $N_0 = 0$, we find that for $k \geq 1$ the elements of the pulse sequence N_k are determined by the formula

$$N_k = \min_{N > N_{k-1}} \{N \mid d_N < d_{N_{k-1}}\} \tag{27}$$

Using formula (27) together with (26), we immediately obtain the diameter sequence d_{N_k} which, for any fixed λ , is the maximal strictly monotone decreasing subsequence of the sequence d_N .

The remarkable feature of the recursive formula (27) is that it is *universal*, i.e., independent of the concrete form of the Hamiltonian (1) and of the particular weak and strong resonances under consideration. This fact enables us to construct the diameter sequence d_{N_k} in general as a function of the bifurcation parameter λ . We start by selecting an integer $N \geq 1$ and consider the family of lines defined by $d_N = |2l\pi - N\lambda|$, $l \in \mathbb{Z}$, on the (λ, d) plane of $\lambda \in [0, 2\pi)$ and $d > 0$. For any λ we determine the point in this diagram that is the closest to the λ axis and highlight it if it also falls below all points found in this fashion for integers less than N . We show this easy graphical construction in Fig. 7 for $N = 1, 2, 3, 4$ and in Fig. 8 for $N = 1, \dots, 100$. The resulting bifurcation diagram is an infinite binary tree which we shall refer to as the *homoclinic tree*. (A similar binary tree appeared in ref. 16 in the study of a modal truncation of a parametrically forced beam.) In a given example only the part of the tree with $d < d_0$ is meaningful. The nodes of the homoclinic tree correspond to bifurcations in the layer sequence as the parameter λ is varied. These bifurcations occur for rational values of $2\pi/\lambda$ which form a dense set of the parameter space.

Since the gradient of the reduced Hamiltonian is nonzero along the closed orbits in the region \mathcal{D}_0 , there exists a smooth, one-to-one relationship between the angular diameter of the closed orbits and their energy. In other words, there exists a diffeomorphism $f_0: \mathbb{R} \rightarrow \mathbb{R}$ with $f_0(d_{N_k}) = \mathcal{H} \mid \gamma_{N_k}$, where $\gamma_{N_k} \subset \mathcal{D}_0$ is the periodic orbit with angular diameter d_{N_k} . Since the orbits on the manifold \mathcal{M}_ρ are close to the orbits of \mathcal{H} , and they depend smoothly on $\sqrt{\rho}$ for $\rho > 0$, there also exists a diffeomorphism $f_\rho: \mathbb{R} \rightarrow \mathbb{R}$ such that

$$f_\rho(d_{N_k}) = H_{\text{pend}}(\gamma_{N_k}^\rho) = H_{\text{pend}}(0, \alpha_{10}, 0) + \rho \mathcal{H} \mid \gamma_{N_k} + \mathcal{O}(\rho^{3/2})$$

In other words, *there exists an appropriate nonlinear scaling such that the vertical axis of the bifurcation diagram in Fig. 8 becomes just the scaled energy of the bifurcating multipulse orbits.*

In Fig. 9 we also show the pulse sequence $N_k(\lambda)$ determined by (27). As one can see, the possible bifurcations in pulse numbers form a very rich

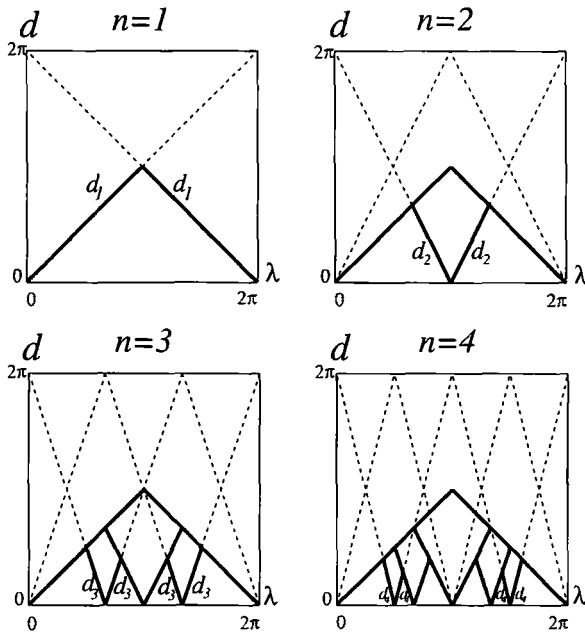


Fig. 7. Geometric construction of the diameter sequence d_{N_k} .

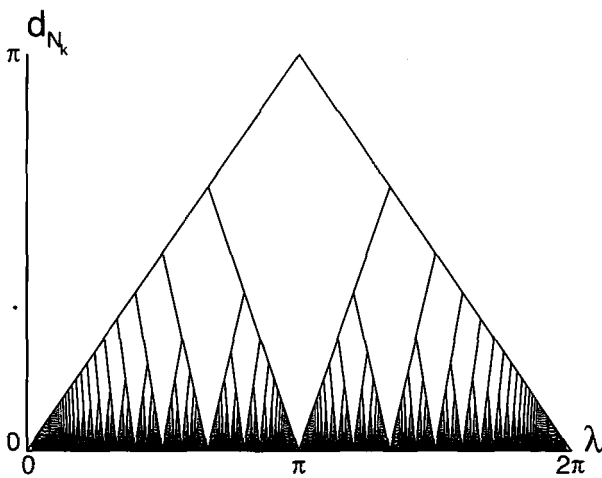


Fig. 8. The universal homoclinic tree for $N_k \leq 100$.

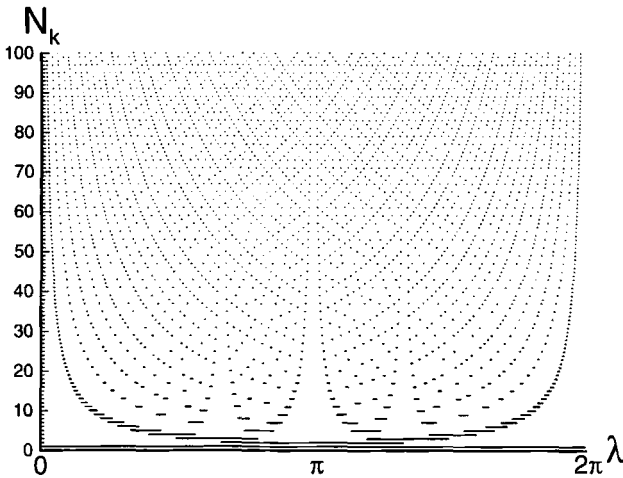


Fig. 9. The universal pulse sequence for $N_k \leq 100$.

family which is not restricted to pulse doubling or tripling. We summarize our main results in the following theorem.

Theorem 3.2. Let us assume that Assumptions (A1) and (A2) are satisfied. Then:

(i) If for all $(\eta, \alpha_2) \notin \mathcal{D}_0$ we have $p_{11}(\mathcal{H}(\eta, \alpha_2) - \mathcal{H} | \gamma_0) < 0$, then, for $\rho > 0$ small enough, there exists a set \mathcal{D}_ρ on the slow manifold close to \mathcal{D}_0 which is filled with slow periodic orbits that admit at least four two-pulse, librational homoclinic orbits.

(ii) If for all $(\eta, \alpha_2) \notin \mathcal{D}_0$ we have $p_{11}(\mathcal{H}(\eta, \alpha_2) - \mathcal{H} | \gamma_0) > 0$, then for any fixed value of the parameter $\lambda(\Delta\alpha_2^+)$, for any element N_k of the corresponding pulse sequence $N_k(\lambda)$ graphed in Fig. 9, and for $\rho > 0$ small enough, the perturbed system (19) has an infinite number of transverse, N_k -pulse rotational orbits homoclinic to slow periodic orbits in the manifold \mathcal{M}_ρ . Accordingly, there exist Smale horseshoes with chaotic dynamics on the energy levels containing these periodic orbits. The slow periodic orbits with N_k -pulse homoclinic orbits form a smooth layer L_{N_k} with inner angular diameter close to d_{N_k} , as graphed in Figs. 7 and 8.

(iii) The maximal splitting angle along the rotational homoclinic orbits in statement (ii) is $\mathcal{O}(\sqrt{\rho})$ as $\rho \rightarrow 0$.

Proof. To prove the theorem we only note that, by Assumption (A2), for any $(\eta, \alpha_2) \notin \mathcal{D}_0$ and for all periodic orbits $\gamma \in \mathcal{D}_0$ we have

$$\text{sign}[p_{11}(\mathcal{H}(\eta, \alpha_2) - \mathcal{H} | \gamma)] = \text{sign}[p_{11}(\mathcal{H}(\eta, \alpha_2) - \mathcal{H} | \gamma_0)]$$

In view of this, the statements of the theorem follow from Theorem 3.1 combined with our previous discussion and the Smale–Birkhoff homoclinic theorem.⁽⁹⁾ ■

Remark 3.3. If the minimal period p of the reduced Hamiltonian is less than 2π , then Assumption (A2) cannot be satisfied, hence Theorem 3.2 is not applicable directly. However, if there exists a periodic orbit γ_0 of the type described in (A2) and it is energetically unique within some annular region $\alpha_2 \in [\hat{\alpha}_2, \hat{\alpha}_2 + p]$, then for phase shift values with $|\Delta\alpha_2^+| \bmod 2\pi < p$ a theorem analogous to Theorem 3.2 can be proven. In general, the multi-pulse orbits obtained in this way will be heteroclinic orbits connecting different slow periodic solutions.

Theorem 3.2 suggests that the dynamics of the pendulum Hamiltonian is more chaotic near the slow manifold if the conditions of (ii) hold than in the case of (i). This follows from the facts that in the case covered by statement (ii) the transversality of the intersecting stable and unstable manifolds is guaranteed at an angle of $\mathcal{O}(\sqrt{\rho})$ and the intersection orbit makes more than two pulses. At the same time, in the case covered by statement (i) we can conclude the existence of an open set of initial conditions that first cross the stronger resonance relatively fast, then cross the weak resonance along the strong one at a much lower speed (see also the related results in ref. 17).

3.3. Passage to the Limit $\rho = \mu$

In this subsection we prove that for μ small enough, i.e., for sufficiently higher weaker resonances, the invariant manifolds and nontrivial homoclinic orbits continue to exist in the pendulum Hamiltonian $H_{\text{pend}}(A, \alpha; \rho)$ even as we increase ρ up to μ . This is important since $H_{\text{pend}}(A, \alpha; \rho)$ is only equal to the original pendulum Hamiltonian in (6) if we set $\rho = \mu$. We can prove the following result.

Theorem 3.3. Let us assume that for arbitrary small $\mu_0 > 0$ and for any integer $\bar{N} > 0$ there exist constants $c_3 > 0$ and μ_-, μ_+ with $0 < \mu_- < \mu_+ < \mu_0$ such that for any $\mu \in [\mu_-, \mu_+]$, $0 < N < \bar{N}$, and $\bar{\alpha}_2 \in S^1$ with $\Delta^N \mathcal{H}(\bar{\alpha}_2) = 0$,

$$|D_{\alpha_2} \Delta^N \mathcal{H}(\bar{\alpha}_2)| > c_3 > 0 \tag{28}$$

holds. Then there exists an infinite set $\mathcal{S}_{\bar{N}}$ of closed intervals in any vicinity of zero such that for any $\mu \in \mathcal{S}_{\bar{N}}$ and $N < \bar{N}$, the results listed in Theorems 3.1 and 3.2 remain valid for $\rho = \mu$.

Proof. First we prove that the invariant manifold \mathcal{M}_ρ continues to exist for $\rho = \mu$. To this end, we need to verify that the manifold \mathcal{M}_ρ is normally hyperbolic^(9,21) for all ρ with $0 \leq \rho \leq \mu$. This requires the computation of the Lyapunov type numbers

$$\begin{aligned} \lambda^u(p) &= \limsup_{t \rightarrow \infty} \| \Pi^u DF_{-t}(\rho) |_{N_\rho^u} \|^{1/t} \\ v^s(p) &= \limsup_{t \rightarrow \infty} \| \Pi^s DF_t[F_{-t}(\rho)] |_{N_\rho^s} \|^{1/t} \\ \sigma^s(p) &= \limsup_{t \rightarrow \infty} \frac{\log \| DF_{-t} |_{\mathcal{M}_\rho(p)} \|}{-\log \| \Pi^s DF_t[F_{-t}(\rho)] |_{N_\rho^s} \|} \end{aligned} \tag{29}$$

where p is an arbitrary point on the manifold \mathcal{M}_ρ , $F_t(\cdot)$ denotes the flow generated by the pendulum Hamiltonian H_{pend} , N_ρ^s and N_ρ^u denote fibers at p in the stable and unstable subbundles, respectively, of the normal bundle of \mathcal{M}_ρ , and the maps $\Pi^s: T\mathbb{R}^2|_{\mathcal{M}_\rho} \rightarrow N^s$ and $\Pi^u: T\mathbb{R}^{2n}|_{\mathcal{M}_\rho} \rightarrow N^u$ denote projections to the stable and unstable subbundles of \mathcal{M}_ρ . From (16) we obtain that for $\rho = 0$ the eigenvalues associated with the linear part of H_{pend} along the manifold \mathcal{M}_0 are $\lambda_{1,2} = \pm [p_{11} D_{x_1}^2 V_1(\alpha_{10}; \mu)]^{1/2}$. Then, in an appropriate basis, the linearized flow operator of (35) takes the form

$$DF_t |_{\mathcal{M}_0} = e^{A_0 t}$$

with $A_0 = \text{diag}(\lambda_1, \lambda_2)$. Direct substitution into (29) gives the type numbers

$$\begin{aligned} \lambda^u(p) &= \exp\{ - [p_{11} D_{x_1}^2 V_1(\alpha_{10}; \mu)]^{1/2} \} \\ v^s(p) &= \exp\{ - [p_{11} D_{x_1}^2 V_1(\alpha_{10}; \mu)]^{1/2} \} \\ \sigma^s(p) &= 0 \end{aligned} \tag{30}$$

which shows that

$$\sup_p \lambda^u(p), \sup_p v^s(p) < 1, \quad \sup_p \sigma^s(p) < 1/r \tag{31}$$

for any integer $r \geq 1$. This just reflects the fact that for $\rho = 0$ the manifold \mathcal{M}_0 is normally hyperbolic. The question is whether the suprema of the type numbers λ^u , λ^s , and σ^s stay bounded away uniformly from 1 and $1/r$, respectively, as we increase the parameter ρ up to μ . By a result of Kopell,⁽²³⁾ for $\rho \geq 0$ and for any fixed $T > 0$, the supremum of the type number λ_ρ^u computed for the perturbed manifold \mathcal{M}_ρ can be estimated as

$$\begin{aligned} \sup_{p \in \mathcal{M}_\rho} \lambda_\rho''(p) &\leq \sup_{p \in \mathcal{M}_\rho} \|II''DF''_{-\tau}(p)\|^{1/\tau} \\ &= \sup_{p \in \mathcal{M}_0} \|II''DF^0_{-\tau}(p)\|^{1/\tau} + \mathcal{O}(\rho) \\ &= \exp\{-[p_{11}D_{x_1}^2 V_1(\alpha_{10}; \mu)]^{1/2}\} + \mathcal{O}(\rho) \\ &\leq \exp(-\sqrt{c_1}) + \mathcal{O}(\rho) \end{aligned}$$

where we used the nondegeneracy condition (13). But this shows that $\sup_{p \in \mathcal{M}_\rho} \lambda_\rho''(p) < 1$ holds for all $\rho \leq \mu$ if $\mu > 0$ is sufficiently small. A similar argument shows that the rest of the inequalities in (1) also hold for all $\rho \leq \mu$. This implies the existence of a normally hyperbolic invariant manifold \mathcal{M}_μ which is $\mathcal{O}(\mu)$ C^r -close to \mathcal{M}_0 and admits stable and unstable manifolds C^r -close to those of \mathcal{M}_0 .

The next step is to verify the persistence of multipulse orbits described in Theorems 3.1 and 3.2. In the (sketchy) proof of Theorem 3.1 we gave a geometric formulation of the problem of existence of multipulse solutions. A more analytic approach (see, e.g., ref. 18) yields that N -pulse homoclinic orbits correspond to transverse zeros of the energy-difference equation

$$\Delta^N \mathcal{H}(\alpha_2) + \delta_0 \mathcal{F}_N(\alpha_2, \eta, \rho^\tau) + \rho^\tau \mathcal{G}_N(\alpha_2, \eta, \rho^\tau) = 0 \tag{32}$$

where the function $\Delta^N \mathcal{H}$ is defined in (23), \mathcal{F}_N and \mathcal{G}_N are smooth functions, $1/2 < \tau < 1$, and $\delta_0 > 0$ is an arbitrarily small constant which is independent of ρ , i.e., remains unchanged as $\rho \rightarrow 0$. The right-hand side of the above equation is equal to $[H_{\text{pend}}(s_N) - H_{\text{pend}}(p_N)]/\varepsilon$, where p_N is a point in the N th intersection of $W''(\mathcal{M}_\mu)$ with a three-dimensional cylinder U_{δ_0} of radius δ_0 centered around \mathcal{M}_ρ . The point s_N lies in $W''_{\text{loc}}(\mathcal{M}_\rho)$ and its η and α_2 coordinates are the same as those of p_N . It is shown in ref. 18 that if the energies of s_N and p_N are the same, then the two points coincide, giving rise to an N -pulse orbit homoclinic to \mathcal{M}_ρ . Clearly, transverse zeros $\bar{\alpha}_2$ of the energy-difference function $\Delta^N \mathcal{H}$ given rise to zeros $\bar{\alpha}_2(\rho)$ of Eq. (32) for $\rho > 0$ small enough by the implicit function theorem. We want to show that these zeros persist as we increase ρ up to μ .

By the meaning of the right-hand side of (32) explained above, the functions \mathcal{F}_N and \mathcal{G}_N are periodic in the variable α_2 and their η dependence comes from the kinetic energy term $\langle A, PA \rangle$ of the pendulum Hamiltonian H_{pend} . This fact together with the estimate (8) implies that for a fixed compact set of I' values and for $0 < N < \bar{N}$ we have

$$|D_{x_2} \mathcal{F}_N|, |D_{x_2} \mathcal{G}_N| < c_4 \left(\log \frac{1}{\mu} \right)^2 \tag{33}$$

for some constant $c_4 > 0$. Selecting $\delta_0 = \mu^\tau$, we can use estimate (33) together with condition (28) of the theorem to conclude that for μ values from intervals of the form $[\mu_-, \mu_+]$,

$$\begin{aligned}
 & |D_{x_2}[\Delta^N \mathcal{H}(\bar{\alpha}_2(\rho)) + \delta_0 \mathcal{F}_N(\bar{\alpha}_2(\rho), \eta, \rho^\tau) + \rho^\tau \mathcal{G}_N(\bar{\alpha}_2(\rho), \eta, \rho^\tau)]| \\
 & \geq c_3 - 2c_4 \mu^\tau \left(\log \frac{1}{\mu}\right)^2 > \frac{c_3}{2} > 0
 \end{aligned}
 \tag{34}$$

uniformly in $\rho \leq \mu$ provided $\mu > 0$ is small enough. But then the implicit function theorem implies that the local solution $\bar{\alpha}_2(\rho)$ of Eq. (32) can be continued up to $\rho = \mu$. Then the statement about persisting invariant Cantor sets follows from the persistence of transverse homoclinic orbits for $\rho = \mu$. Finally, the maximal splitting angle is continuous in the parameter ρ , since the intersecting stable and unstable manifolds are continuous in ρ . This proves that the maximal splitting angle along N -pulse rotational homoclinic orbits is $\mathcal{O}(\sqrt{\mu})$ in the limit $\rho = \mu$. ■

We note that assumption (28) of the above theorem means that arbitrarily close to the origin of the μ axis we can find intervals for which the order of transversality of the zeros of a finite number of energy difference functions $\Delta^N \mathcal{H}$ is independent of μ . Since the entries of the matrix P typically depend on μ as $[\log(1/\mu)]^2$ [see estimate (8)], the value of $\Delta \alpha_2^+ \bmod 2\pi$ runs through S^1 repeatedly as μ becomes smaller and smaller [see (18)]. Still, we can find a set \mathcal{S}_N of intervals on the μ axis within which

$$D_{x_2} \Delta^N \mathcal{H}(\bar{\alpha}_2) = D_{x_2} [V_2(\alpha_{10}, \alpha_2 + N \Delta \alpha_2^+(\mu); \mu) - V_2(\alpha_{10}, \alpha_2; \mu)]$$

stays bounded away from zero uniformly in μ . In our example in Section 5 we in fact obtain that \mathcal{S}_N can be taken a single connected interval of the form $(0, \mu_0]$.

4. DYNAMICS IN THE NORMAL FORM

In this section we extend the results obtained for H_{pend} to the full normal form Hamiltonian $H(A, \alpha, B, \beta)$ defined in (5). As a first step, we assume that condition (28) holds and fix $\bar{N} > 0$ and $\mu \in \mathcal{S}_{\bar{N}}$ (see Theorem 3.3). Then for any higher order resonance with $|r_2| > L(\mu)$ that intersects the fixed strong resonance with generator r_1 , the invariant manifolds and multipulse homoclinic orbits described in the previous section exist.

4.1. The Truncated Normal Form

We now describe the invariant manifolds of the truncated n -degree-of-freedom normal form that correspond to the invariant manifolds of the pendulum equation. It is easy to see that any k -dimensional invariant manifold M of the Hamiltonian H_{pend} gives rise to a $[k + 2(n - 2)]$ -dimensional invariant manifold \bar{M} for the truncated normal form Hamiltonian

$$\bar{H}(A, \alpha, B; \varepsilon) = \sqrt{\varepsilon} [H_{\text{pend}}(A, \alpha) + \sqrt{\varepsilon} H_2(A, \alpha, B; \sqrt{\varepsilon})] \tag{35}$$

which generates the Hamiltonian vector field

$$\begin{aligned} \dot{\alpha} &= \sqrt{\varepsilon} D_A [H_{\text{pend}}(A, \alpha) + \sqrt{\varepsilon} H_2(A, \alpha, B; \sqrt{\varepsilon})] \\ \dot{A} &= -\sqrt{\varepsilon} D_\alpha [H_{\text{pend}}(A, \alpha) + \sqrt{\varepsilon} H_2(A, \alpha, B; \sqrt{\varepsilon})] \\ \dot{\beta} &= b + \sqrt{\varepsilon} D_B H_2(A, \alpha, B; \sqrt{\varepsilon}) \\ \dot{B} &= 0 \end{aligned}$$

through the symplectic form ω defined in (11). The manifold \bar{M} is diffeomorphic to $M \times U \times \mathbb{T}^{n-2}$, where $U \subset \mathbb{R}^{n-2}$ is an open subset of the space of the action variables B . In particular, under the assumptions of Section 3, the truncated Hamiltonian \bar{H} admits a $(2n - 2)$ -dimensional invariant manifold of the form

$$\bar{M}_\mu = \left\{ (A, \alpha, B, \beta) \mid \alpha_1 = \alpha_{10} + \mathcal{O}(\sqrt{\mu}), A_1 = -\frac{p_{12}}{p_{11}} A_2 + \mathcal{O}(\sqrt{\mu}), B \in U \right\} \tag{36}$$

\bar{M}_μ contains an open set \bar{D}_μ diffeomorphic to $\mathcal{D}_\mu \times U \times \mathbb{T}^{n-2}$. (Note that these invariant manifolds intersect different energy surfaces: fixing the energy would reduce their dimensions by one.)

Now let us consider a periodic solution $\gamma \subset \mathcal{D}_\mu \subset \bar{M}_\mu$ which has an N -pulse homoclinic orbit y^N . Fixing the integrals (B_1, \dots, B_{n-2}) in the truncated normal form, we see that γ gives rise to an $(n - 1)$ -dimensional torus $\Gamma = \gamma \times \mathbb{T}^{n-2}$. One frequency on this torus is $\mathcal{O}(\sqrt{\mu\varepsilon})$ and the rest are $\mathcal{O}(1)$. The torus admits n -dimensional stable and unstable manifolds given by $W^{s,u}(\Gamma) = W^{s,u}(\gamma) \times \mathbb{T}^{n-2}$. These manifolds intersect in the $(n - 1)$ -dimensional homoclinic set $y^N \times \mathbb{T}^{n-2}$. By a simple dimension count, the intersection of $W^s(\Gamma)$ is not transverse within the $(2n - 1)$ -dimensional energy surface (recall that $n \geq 3$). In particular, the splitting distance between the manifolds $W^s(\Gamma)$ and $W^u(\Gamma)$ is zero when measured in the direction of the action variables (B, β) . At the same time, in the case

covered by statement (ii) of Theorem 3.2, the splitting distance and the maximal splitting angle of these manifolds is $\mathcal{O}(\sqrt{\mu})$ in the (A, α) directions, as we stated in Theorem 3.3 (cf. Remark 3.2). Consequently, the splitting matrix M_p defined in (24) can be chosen in such a way that one diagonal element is $\mathcal{O}(\sqrt{\mu})$ and all the other entries are zero. Since the norm of this matrix is $\mathcal{O}(\sqrt{\mu})$, we find that the maximal splitting angle is $\mathcal{O}(\sqrt{\mu})$. Passing back to the original action-angle variables (I, ϕ) , we then obtain that the maximal splitting angle is $\mathcal{O}(\sqrt{\mu\varepsilon})$. Fixing $\mu > 0$ then shows that the maximal splitting angle for the stable and unstable manifolds of the $(n-1)$ -tori of the truncated normal form is $\mathcal{O}(\sqrt{\varepsilon})$ as $\varepsilon \rightarrow 0$, when we measure the angle in terms of the original (I, ϕ) variables.

If the conditions of (ii) of Theorem 3.2 are satisfied, then we immediately obtain invariant Cantor sets with chaotic dynamics for a Poincaré map associated with the truncated Hamiltonian \bar{H} . These Cantor sets are the Cartesian products of the Cantor sets obtained in the theorem with the set $U \times \mathbb{T}^{n-2}$.

4.2. The Full Normal Form

The following theorem describes how the above structures survive in the full normal form (5).

Theorem 4.1. Suppose that Assumptions (1) and (A2) are satisfied uniformly for $\mu > 0$ small enough. Then for any $\bar{N} > 0$ and $\mu \in \mathcal{S}_{\bar{N}}$ sufficiently small there exists $\varepsilon_0 > 0$ such that for $0 < \varepsilon < \varepsilon_0$:

(i) The Hamiltonian system (5) has a $(2n-2)$ -dimensional invariant manifold M_μ which is $\mathcal{O}(\sqrt{\varepsilon})$ C^r -close to \bar{M}_μ for any finite integer $r \geq 1$. The manifold M_μ has $(2n-1)$ -dimensional stable and unstable manifolds which are $\mathcal{O}(\sqrt{\varepsilon})$ C^r -close to $W^s(\bar{M}_\mu)$ and $W^u(\bar{M}_\mu)$, respectively, in a neighborhood of M_μ . (Fixing the energy would reduce the dimensions of these manifolds by one.)

(ii) If for all $(\eta, \alpha_2) \notin \mathcal{D}_0$ we have $p_{11}(\mathcal{H}(\eta, \alpha_2) - \mathcal{H} | \gamma_0) > 0$, then for any fixed value of the parameter $\lambda(\Delta\alpha_2^+)$ and for any element $N_k < \bar{N}$ of the corresponding pulse sequence $N_k(\lambda)$ (graphed in Fig. 9) the normal form (5) has an infinite number of N_k -pulse rotational orbits homoclinic to a set $D_\mu \subset M_\mu$ which is diffeomorphic to $\mathcal{D}_0 \times U \times \mathbb{T}^{n-2}$. The N_k -pulse orbits are asymptotic to solutions which stay in the set $L_{N_k} \times U \times \mathbb{T}^{n-2} \subset M_\mu$ for times $\mathcal{O}(\log 1/\sqrt{\varepsilon})$ [cf. (ii) of Theorem 3.2].

(iii) The maximal splitting angle along the rotational homoclinic orbits in statement (iii) is $\mathcal{O}(\sqrt{\varepsilon})$ as $\varepsilon \rightarrow 0$.

(iv) An appropriately defined Poincaré map associated with (5) possesses an invariant Cantor set with chaotic dynamics whose elements are diffeomorphic to the set $U \times \mathbb{T}^{n-1}$.

Proof. Just as in Theorem 3.3, we prove (i) by verifying that the manifold \bar{M}_μ is normally hyperbolic. A similar calculation shows that the Lyapunov type numbers for \bar{M}_μ are of the form

$$\begin{aligned} \lambda^u(p) &= \exp\{-[\varepsilon p_{11} D_{\alpha_1}^2 V_1(\alpha_{10}; \mu)]^{1/2}\} + \mathcal{O}(\mu) \\ v^s(p) &= \exp\{-[\varepsilon p_{11} D_{\alpha_1}^2 V_1(\alpha_{10}; \mu)]^{1/2}\} + \mathcal{O}(\mu) \\ \sigma^s(p) &= 0 \end{aligned}$$

which again yields that

$$\sup_p \lambda^u(p), \sup_p v^s(p) < 1, \quad \sup_p \sigma^s(p) < 1/r$$

for any integer $r \geq 1$ and for $\varepsilon, \mu > 0$ small enough. This means that for $\varepsilon > 0$ and for $\mu > 0$ small enough the manifold \bar{M}_μ is normally hyperbolic and any Hamiltonian sufficiently close to \bar{H} possesses a nearby invariant manifold M_μ with the properties described in statement (i) of the theorem. However, for fixed ε the exponentially small “tail” of the normal form Hamiltonian (5) means a perturbation of fixed size on the manifold \bar{M}_μ . In other words, the strength of the hyperbolicity of \bar{M}_μ depends on the perturbation parameter ε . To resolve this difficulty, we follow the same approach as in the proof of Theorem 3.3 by introducing an auxiliary perturbation parameter $\hat{\varepsilon}$ and considering the Hamiltonian

$$\begin{aligned} \hat{H}(A, \alpha, B, \beta; \hat{\varepsilon}) &= \sqrt{\hat{\varepsilon}} \langle b, B \rangle + \sqrt{\hat{\varepsilon}} [H_{\text{pend}}(A, \alpha) + \sqrt{\hat{\varepsilon}} H_2(A, \alpha, B; \sqrt{\hat{\varepsilon}})] \\ &\quad + \hat{\varepsilon} H_3(A, \alpha, B, \beta; \sqrt{\hat{\varepsilon}}) \end{aligned} \tag{37}$$

for some fixed, sufficiently small value of $\hat{\varepsilon}$. By the normal hyperbolicity of \bar{M}_μ , there exists $\hat{\varepsilon}_0 > 0$ such that for all $0 < \hat{\varepsilon} < \hat{\varepsilon}_0$ the Hamiltonian system generated by \hat{H} admits an invariant manifold $M_\mu^{\hat{\varepsilon}}$ with the desired properties. For any such $\hat{\varepsilon}$ this manifold is normally hyperbolic; hence $\hat{\varepsilon}$ can be slightly increased and $M_\mu^{\hat{\varepsilon}}$ persists. We would like to argue that it is possible to increase $\hat{\varepsilon}$ up to $\exp(-c/\varepsilon^v)$ and preserve the normal hyperbolicity of $M_\mu^{\hat{\varepsilon}}$ [i.e., preserve the inequalities (31) for the type numbers computed for $M_\mu^{\hat{\varepsilon}}$]. By the result from Kopell⁽²³⁾ that we used in the proof of Theorem 3.3, for any fixed $T > 0$ the supremum of the type number $\lambda_{\hat{\varepsilon}}^u$ computed for the perturbed manifold $M_\mu^{\hat{\varepsilon}}$ obeys the estimate

$$\begin{aligned}
 \sup_{p \in M_\mu^\varepsilon} \lambda_{\hat{\varepsilon}}^u(p) &\leq \sup_{p \in M_\mu^\varepsilon} \|H^u DF_{-T}^\varepsilon(p)\|^{1/T} \\
 &= \sup_{p \in M_\mu} \|H^u DF_{-T}^0(p)\|^{1/T} + \mathcal{O}(\hat{\varepsilon}) \\
 &= \exp\{-[\varepsilon p_{11} D_{\alpha_1}^2 V_1(\alpha_{10}; \mu)]^{1/2}\} + \mathcal{O}(\mu, \hat{\varepsilon}) \\
 &< \exp(-\sqrt{\varepsilon c_3}) + \mathcal{O}(\mu, \hat{\varepsilon})
 \end{aligned}$$

hence

$$\sup_{p \in M_\mu^\varepsilon} \lambda_{\hat{\varepsilon}}^u(p) < 1$$

holds for all $\hat{\varepsilon} \leq \exp(-c/\varepsilon^v)$. A similar argument shows that the rest of the inequalities in (1) also hold for all $\hat{\varepsilon} \leq \exp(-c/\varepsilon^v)$, which proves statement (i). The persistence of multipulse orbits and their properties follow from Theorems 3.2 and 3.3 and from the fact that exponentially small perturbations preserve the transverse intersections of the stable and unstable manifolds of M_μ which intersect at an angle $\mathcal{O}(\mu)$. Finally, the statement about persisting invariant Cantor sets follows from the structural stability of invariant sets of the truncated normal form, which are Cartesian products of Smale horseshoes with the set $U \times \mathbb{T}^{n-2}$. ■

The above theorem does not state that the surviving multipulse orbits are still asymptotic to whiskered tori which are contained in the persisting $(2n - 2)$ -dimensional manifold M_μ . While this statement is most likely true, it cannot be proven by the direct applications of the existing versions of the KAM theory. In particular, the results of Moser,⁽²⁸⁾ Graff,⁽¹³⁾ or Zehnder^(34,35) do not apply here since the Lyapunov exponents are not constant along the unperturbed whiskered tori. Similarly, a direct application of the KAM theorem to the dynamics on the symplectic manifold M_μ is not possible since the restricted symplectic form is noncanonical. As a result, the restricted Hamiltonian vector field cannot be written in a near-integrable form in any obvious way. Nevertheless, the multipulse solutions constructed above remain exponentially close to invariant whiskered tori of the truncated normal form on time scales $\mathcal{O}(\exp(c/\varepsilon^v))$. Thus, for numerical purposes, their actual limit sets are indistinguishable from $(n - 1)$ -dimensional invariant tori.

5. AN EXAMPLE

In this section we illustrate our general results on the three-degree-of-freedom mechanical model shown in Fig. 1. The positions of the three disks

in this system are measured by the angles δ_1 , δ_2 , and δ_3 . The first disk on the top is attached to the upper fixed shaft via a torsional spring of stiffness s_1 as well as to the second disk via a linear spring of stiffness s_2 . The third disk at the bottom is also attached to the second disk via a linear spring of stiffness s_3 . The unstretched lengths of the two linear springs are l_{10} and l_{20} , respectively, and their endpoints on the first and the third disks have eccentricities εr_1 and εr_2 , respectively, where $\varepsilon \geq 0$ is a small parameter. (For $\varepsilon = 0$ the three disks decouple from each other.) The endpoints of the two linear springs on the second body lie at a distance of R from the shaft, and we assume that $l_{10}, l_{20} < R$. The moments of inertia of the three bodies with respect to the common axis of rotation are denoted by \mathcal{I}_1 , \mathcal{I}_2 , and \mathcal{I}_3 , respectively.

It is easy to verify that the kinetic energy T and the potential energy V of this three-degree-of-freedom system are given by

$$T = \frac{1}{2} \mathcal{I}_1 \dot{\delta}_1^2 + \frac{1}{2} \mathcal{I}_2 \dot{\delta}_2^2 + \frac{1}{2} \mathcal{I}_3 \dot{\delta}_3^2$$

$$V = \frac{1}{2} s_1 \delta_1^2 - \varepsilon [s_1 r_1 (R - l_{10}) \cos(\delta_2 - \delta_1) + s_1 r_2 (R - l_{20}) \cos(\delta_2 - \delta_3)] + \mathcal{O}(\varepsilon^2)$$

We introduce action-angle variables $I_i, \phi_i, i = 1, 2, 3$, by letting

$$\delta_1 = \sqrt{2I_1 \frac{\omega_1}{s_1}} \sin \phi_1, \quad \dot{\delta}_1 = \frac{1}{\mathcal{I}_1} \sqrt{2I_1 \frac{s_1}{\omega_1}} \cos \phi_1$$

$$\phi_2 = \delta_2, \quad I_2 = \mathcal{I}_2 \dot{\delta}_2, \quad \phi_3 = \delta_3, \quad I_3 = \mathcal{I}_3 \dot{\delta}_3$$

where $\omega_1 = \sqrt{s_1/\mathcal{I}_1}$ is the torsional natural frequency for the free oscillations of the first body. In these new variable the Hamiltonian $H = T + V$ can be written as

$$H(I, \phi; \varepsilon) = H_0(I) + \varepsilon H_1(I, \phi; \varepsilon)$$

with

$$H_0(I) = \omega_1 I_1 + \frac{1}{2} \frac{I_2^2}{\mathcal{I}_2} + \frac{1}{2} \frac{I_3^2}{\mathcal{I}_3} \tag{38}$$

$$H_1(I, \phi; \varepsilon) = -\varepsilon \left[s_1 r_1 (R - l_{10}) \cos \left(\phi_2 - \sqrt{2I_1 \frac{\omega_1}{s_1}} \sin \phi_1 \right) + s_2 r_2 (R - l_{20}) \cos(\phi_2 - \phi_3) \right] + \mathcal{O}(\varepsilon^2) \tag{39}$$

For $|\text{Im } z_1|, |\text{Im } z_2|, |\text{Im } z_3| < \sigma$ the modulus of the complex extended Hamiltonian $H_1(I, z; \varepsilon)$ can be estimated as $|H_1(I, z; \varepsilon)| < K_\sigma$ with

$$K_\sigma = 2 + s_2 r_2 (R - l_{20}) (1 + \sinh^2 2\sigma)^{1/2} + s_1 r_1 (R - l_{10}) \left\{ 1 + \sinh^2 \left[\sigma + \left(2I_1 \frac{\omega_1}{s_1} \right)^{1/2} \sinh \sigma \right] \right\}^{1/2} \quad (40)$$

where we used some elementary identities for hyperbolic functions.

We are interested in motions of the model near a double resonance where

$$\dot{\phi}_2 = \dot{\phi}_3, \quad k_1 \dot{\phi}_1 = \dot{\phi}_2$$

holds for $\varepsilon = 0$ and for some $k_1 \in \mathbb{Z}^+$. On any unperturbed energy surface $H_0(I) = h_0$, this resonance occurs at the action value I' given by

$$I'_1 = \frac{h_0 + \frac{1}{2}(I'_2)^2/\mathcal{J}_2 - \frac{1}{2}(I'_3)^2/\mathcal{J}_3}{\omega_1}, \quad I'_2 = k_1 \omega_1 \mathcal{J}_2, \quad I'_3 = k_1 \omega_1 \mathcal{J}_3 \quad (41)$$

Since we assume a strong 1:1 resonance between the second and the third body, to apply the results of the previous sections we shall need to pick k_1 so that the order of the second 1: k_1 resonance is sufficiently higher than 2.

It is a simple exercise to verify that

$$r_1 = (0, 1, -1), \quad r_2 = (k_1, -1, 0)$$

form a “minimal” basis for the corresponding resonant module M in the sense described after formula (3). We can therefore choose the nonsingular integer matrix

$$T = \begin{pmatrix} 0 & 1 & -1 \\ k_1 & -1 & 0 \\ 1 & 0 & 0 \end{pmatrix}$$

with $\det T = -1$, and obtain the pendulum Hamiltonian (6) in the form

$$H_{\text{pend}}(A, \alpha) = \frac{1}{2} \langle A, PA \rangle + V_1(\alpha_1; \mu) + \mu V_2(\alpha; \mu) \quad (42)$$

with

$$P = \begin{pmatrix} 1/\mathcal{J}_2 + 1/\mathcal{J}_3 & -1/\mathcal{J}_2 \\ -1/\mathcal{J}_2 & 1/\mathcal{J}_2 \end{pmatrix}, \quad V_1(\alpha_1) = -s_2 r_2 (R - l_{20}) \cos \alpha_1 \quad (43)$$

$$V_2(\alpha; \mu) = - \sum_{|p_2 r_2| > L(\mu)} s_1 r_1 (R - l_{10}) \frac{\tilde{h}_{(0, p_2)}}{\mu} \cos p_2 \alpha_2$$

where

$$\tilde{h}_{(0, p_2)} = \frac{1}{4\pi^2} \int_0^{2\pi} \int_0^{2\pi} \cos \left[\phi_2 - \left(2I_1^r \frac{\omega_1}{s_1} \right)^{1/2} \sin \phi_1 \right] \cos p_2 (k_1 \phi_1 - \phi_2) d\phi_1 d\phi_2 \quad (44)$$

$$L(\mu) = \text{Int} \left[\frac{8}{3\sigma} \log \frac{1}{\mu} + \frac{8}{3\sigma} \log \frac{2^{16} K_\sigma}{27 e^2 \sigma^3} \right] + 1$$

$$= \text{Int} \left[\frac{8}{3\sigma} \log \frac{1}{\mu} + L_0(\sigma) \right] + 1$$

$$L_0(\sigma) = \frac{8}{3\sigma} \log \left\{ \left[2^{16} (2 + s_2 r_2 (R - l_{20}) (1 + \sinh^2 2\sigma))^{1/2} + s_1 r_1 (R - l_{10}) \left\{ 1 + \sinh^2 \left[\sigma + \left(2I_1^r \frac{\omega_1}{s_1} \right)^{1/2} \sinh \sigma \right] \right\}^{1/2} \right] \times (27 e^2 \sigma^3)^{-1} \right\}$$

Here we used the expressions (4) with $\kappa = 3\sigma/4$, (7), (9), and (40). Let $\sigma_0 > 0$ be the point where the function $L_0(\sigma)$ reaches its global minimum on the interval $(0, \infty)$. For this choice of σ the function $L(\mu)$ can be rewritten as

$$L(\mu) = \text{Int} \left[\frac{8}{3\sigma_0} \log \frac{1}{\mu} + L_0(\sigma_0) \right] + 1$$

and the second inequality in (4) is satisfied if for sufficiently small, fixed μ with

$$0 < \mu \ll c_0 = \frac{2}{3} s_2 r_2 (R - l_{20}) \quad (45)$$

the weaker resonance satisfies

$$k_1 \geq \text{Int} \left[\frac{8}{3\sigma_0} \log \frac{1}{\mu} + L_0(\sigma_0) \right] \tag{46}$$

Clearly, for any fixed μ satisfying (45), there is an infinite number of weaker resonances for which (46) holds. For example, for a parameter configuration with

$$s_2 r_2 (R - l_{20}) = s_1 r_1 (R - l_{10}) = 0.01, \quad \left(2I_1^r \frac{\omega_1}{s_1} \right)^{1/2} = 1$$

the graph of $L_0(\sigma)$ near its global minimum is shown in Fig. 10. In this case, as seen from the figure, we have $\sigma_0 \approx 2.21$ and $L_0(\sigma_0) = 7$. Then (46) shows that our analysis is valid near resonance intersections where the weaker resonance satisfies

$$k_1 \geq \text{Int} \left[\frac{4}{3} \log \frac{1}{\mu} + 7 \right]$$

For example, $\mu = 0.001$ would require $k_1 \geq 16$. (As numerical experiments related to the application of the energy-phase method indicate, the multi-pulse orbits generally continue to exist for μ values much higher than 0.001; hence, most likely, lower values of k_1 can also be allowed).

To simplify our calculations, we now restrict our attention to higher order resonances for which the lowest order term in the potential V_2

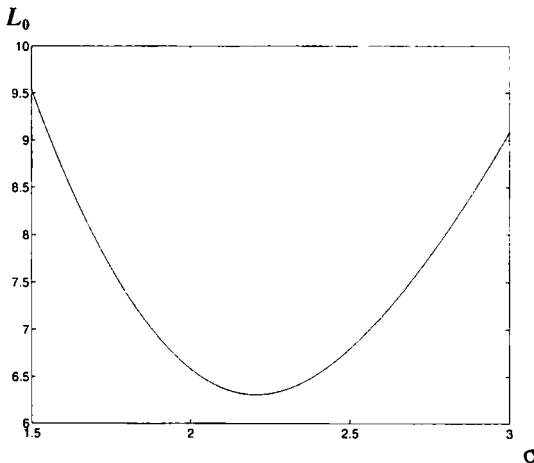


Fig. 10. The graph of the function $L_0(\sigma)$.

dominates the higher order terms. By the exponential decay of the Fourier series of V_2 , this is satisfied for sufficiently large values of k_1 provided the lowest order Fourier coefficient of V_2 is nonzero. To avoid lengthy calculations, we only consider cases when this fact is simple to establish.

Lemma 5.1. Let us suppose that $k_1 = 4l$ with $l \in \mathbb{Z}^+$, and the resonant action value I' lies on an unperturbed energy surface $H_0(I) = h_0$ such that

$$\left(2I'_1 \frac{\omega_1}{s_1}\right)^{1/2} = \left[\frac{2}{s_1} \left(h_0 + k_1^2 s_1 \frac{\mathcal{J}_2 - \mathcal{J}_3}{\mathcal{J}_1}\right)\right]^{1/2} \leq \frac{\pi}{2} \tag{47}$$

Then $\tilde{h}_{(0,1)} < 0$ holds.

Proof. From (44) we obtain that

$$\begin{aligned} \tilde{h}_{(0,1)} = & \frac{1}{4\pi^2} \int_0^{2\pi} \cos \phi_2 \cos \phi_2 d\phi_2 \int_0^{2\pi} \cos k_1 \phi_1 \cos \left[\left(2I'_1 \frac{\omega_1}{s_1}\right)^{1/2} \sin \phi_1 \right] d\phi_1 \\ & + \frac{1}{4\pi^2} \int_0^{2\pi} \sin \phi_2 \sin \phi_2 d\phi_2 \int_0^{2\pi} \sin k_1 \phi_1 \sin \left[\left(2I'_1 \frac{\omega_1}{s_1}\right)^{1/2} \sin \phi_1 \right] d\phi_1 \end{aligned} \tag{48}$$

This expression can be rewritten as

$$\begin{aligned} \tilde{h}_{(0,1)} = & \frac{1}{2\pi} \int_0^\pi \cos k_1 \phi_1 \cos \left[\left(2I'_1 \frac{\omega_1}{s_1}\right)^{1/2} \sin \phi_1 \right] d\phi_1 \\ & + \frac{1}{2\pi} \int_0^\pi \sin k_1 \phi_1 \sin \left[\left(2I'_1 \frac{\omega_1}{s_1}\right)^{1/2} \sin \phi_1 \right] d\phi_1 \end{aligned} \tag{49}$$

where we used the fact that the second factors in both terms in (48) have integrands which are even with respect to $\phi_1 = \pi$. Since the first integrand in (49) is odd and the second integrand is even with respect to $\phi_1 = \pi/2$, we obtain

$$\tilde{h}_{(0,1)} = \frac{1}{\pi} \int_0^{\pi/2} \sin k_1 \phi_1 \sin \left[\left(2I'_1 \frac{\omega_1}{s_1}\right)^{1/2} \sin \phi_1 \right] d\phi_1$$

If $k_1 = 4l$ with $l \in \mathbb{Z}^+$, then this integral can be written as

$$\tilde{h}_{(0,1)} = \frac{1}{\pi} \sum_{m=0}^{k_1-1} \int_{m\pi/k_1}^{(m+1)\pi/k_1} \sin k_1 \phi_1 \sin \left[\left(2I'_1 \frac{\omega_1}{s_1}\right)^{1/2} \sin \phi_1 \right] d\phi_1 \tag{50}$$

By condition (47) the second factor in these integrands is positive and strictly monotone increasing on the interval $[0, \pi/2)$. As a result we obtain

$$\int_{2j\pi/k_1}^{(2j+1)\pi/k_1} \sin k_1 \phi_1 \sin \left[\left(2I_1^r \frac{\omega_1}{s_1} \right)^{1/2} \sin \phi_1 \right] d\phi_1 + \int_{(2j+1)\pi/k_1}^{(2j+2)\pi/k_1} \sin k_1 \phi_1 \sin \left[\left(2I_1^r \frac{\omega_1}{s_1} \right)^{1/2} \sin \phi_1 \right] d\phi_1 < 0$$

for $j=0, \dots, l-1$. But this together with (50) implies the statement of the lemma. ■

The exponential decay of the Fourier coefficients of V_2 and Lemma 5.1 imply that for any $\delta > 0$ small there exists $l_0(\delta) \in \mathbb{Z}^+$ such that for $l > l_0(\delta)$, $k_1 = 4l > L(\mu) - 1$, the potential V_2 can be written as

$$V_2(\alpha; \mu) = \Gamma \cos \alpha_2 + \mathcal{O}(\delta), \quad \Gamma = -s_1 r_1 (R - l_{10}) \frac{\tilde{h}_{(0,1)}}{\mu} > 0 \quad (51)$$

provided condition (47) is satisfied.

We are now in the position to verify the basic assumptions of Section 3 for our example. First, it is easy to see from (43) that

$$p_{11} = \frac{1}{\mathcal{J}_2} + \frac{1}{\mathcal{J}_3}, \quad \det P = \frac{1}{\mathcal{J}_2 \mathcal{J}_3} \quad (52)$$

hence the nondegeneracy conditions in (13) and (14) are satisfied. Furthermore, since p_{11} and V_1 do not depend on μ , our analysis is valid without restricting the resonant action value I^r to a fixed, bounded set (see Remark 2.1).

For $A_2 = 0$, $\alpha_{10} = \pi$ is a saddle-type equilibrium for the unperturbed (α_1, A_1) equations [see (16)]

$$\dot{\alpha}_1 = \left(\frac{1}{\mathcal{J}_2} + \frac{1}{\mathcal{J}_3} \right) A_1 - \frac{1}{\mathcal{J}_2} A_2$$

$$\dot{A}_1 = -s_2 r_2 (R - l_{20}) \sin \alpha_1$$

Since α_{10} is also a unique global maximum for the potential V_1 assumption (1) is satisfied.

Using (51), we can write the reduced Hamiltonian \mathcal{H} in (22) as

$$\mathcal{H}(\eta, \alpha_2; \delta) = \frac{1}{2(\mathcal{J}_2 + \mathcal{J}_3)} \eta^2 + \Gamma \cos \alpha_2 + \mathcal{O}(\delta) \quad (53)$$

whose phase portrait for $\delta = 0$ is just that of the ordinary pendulum. Note that any periodic orbit γ_0 inside the pendulum separatrices satisfies Assumption (A2) of Section 3. Since separatrices are homoclinic orbits on the cylindrical phase space of \mathcal{H} , they and the periodic orbits they encircle are structurally stable with respect to small $\mathcal{O}(\delta)$ Hamiltonian perturbations that are periodic in the variable α_2 . Thus, for $\delta > 0$ small enough, the angular diameter of the domain \mathcal{D}_0^δ (see Fig. 4b) is given by

$$d_0^\delta = 2\pi - \mathcal{O}(\delta)$$

The phase shift $\Delta\alpha_2^+$ defined in (18) takes the form $\Delta\alpha_2^+ = -2\pi(1 + \mathcal{I}_3/\mathcal{I}_2)$, which implies that

$$\lambda = |\Delta\alpha_2^+ \bmod 2\pi| = 2\pi \frac{\mathcal{I}_3}{\mathcal{I}_2} \bmod 2\pi \tag{54}$$

From (52) and (53) we immediately see that

$$p_{11}(\mathcal{H}(\eta, \alpha_2; \delta) - \mathcal{H} | \gamma_0^\delta) > 0, \quad (\eta, \alpha_2) \notin \mathcal{D}_0^\delta$$

which shows that statement (ii) of Theorem 4.1 applies. Finally, since $\Delta\alpha_2^+$ is independent of the parameter μ , condition (28) can be satisfied uniformly in μ for an open set of the plane of the parameters \mathcal{I}_2 and \mathcal{I}_3 . Hence in the proof of Theorem 3.3 the set \mathcal{S}_N can be chosen a single connected interval of the form $(0, \mu_0]$. Then, using the results of this section combined with Theorem 4.1, we obtain the following result for our mechanical model.

Theorem 5.2. For $\varepsilon = 0$ consider a neighborhood of the intersection of the strong resonance $\dot{\phi}_2 = \dot{\phi}_3$ and the weaker resonance $k_1\dot{\phi}_1 = \dot{\phi}_2$ in the phase space of the unperturbed model Hamiltonian H_0 . Suppose that the action values in this neighborhood lie on unperturbed energy surfaces $H_0(I) = h_0$ that satisfy condition (47). Then the following hold.

(i) For $k_1 = 4l$, $l \in \mathbb{Z}^+$ sufficiently large, for any fixed value of δ in (54), and for any element N_k of the corresponding pulse sequence $N_k(\delta)$ graphed in Fig. 9, the perturbed model system has an infinite number of N_k -pulse rotational orbits homoclinic to a set $D_\mu \subset M_\mu$ near the double resonance. The N_k -pulse orbits are asymptotic to solutions which stay in the set $L_{N_k} \times U \times \mathbb{T}^{n-2} \subset M_\mu$ for times $\mathcal{O}(\log 1/\sqrt{\varepsilon})$ [cf. (ii) of Theorem 3.2].

(ii) The bifurcation diagram for the layers L_{N_k} is given in Fig. 8 and is valid for $d_{N_k} < 2\pi - \mathcal{O}(\delta)$, where $\delta > 0$ is a small number.

(iii) An appropriately defined Poincaré map associated with the perturbed model Hamiltonian possesses an invariant Cantor set with

chaotic dynamics whose elements are diffeomorphic to the product of a Smale horseshoe with the set $U \times \mathbb{T}^{n-2}$.

We note that the multipulse orbits obtained from this theorem are of *rotational* type (cf. Definition 3.2). This means the existence of near-resonant motions of our mechanical system along which the phase difference between the second and third bodies increases several times before the solutions pass through the higher order $1:k_1$ resonance between the first and second bodies. After this passage the phases of the second and third bodies remain “locked” in the strong 1:1 resonance.

6. DISCUSSION

In this paper we have studied the dynamics of weak–strong resonance junctions in n -degree-of-freedom, nearly integrable Hamiltonian systems. Analyzing the corresponding normal form, we have found families of homoclinic orbits which are doubly asymptotic to a $(2n-2)$ -dimensional invariant manifold with two times scales. This manifold is filled with solutions that remain close to $(n-1)$ -dimensional whiskered tori for exponentially long times. The homoclinic orbits we found make repeated departures from and returns to the manifold and may represent three different kinds of motion. For one of these types, the rotational motions, we have shown that without the exponentially small “tail” of the normal form, the maximal splitting angle of stable and unstable whiskers along the solution is $\mathcal{O}(\sqrt{\varepsilon})$ [see statement (iii) of Theorem 4.1]. This amounts to a much more significant chaotic dynamics near weak–strong double resonances than the one caused by exponentially small splittings near single resonances.

We gave explicit conditions under which a given resonance in a given system generates librational, rotational, or passing homoclinic orbits (see Definitions 3.1–3.3). We also showed that as the system parameters are varied, the rotational homoclinic orbits generically undergo a complicated but *universal bifurcation* which can be described by the recursive relations (26), (27). These relations define an infinite binary tree, which we called the *homoclinic tree*. In a three-degree-of-freedom mechanical model of rotating, coupled rigid bodies we explicitly verified the existence of this bifurcation as the model parameters are varied.

We believe that our results together with those in ref. 17 complement the mechanism suggested by Arnold for diffusion near a single resonance. While Arnold’s diffusion concerns trajectories that move exponentially slowly near a single resonance in phase space, we describe what happens to these trajectories when they reach a resonance junction, i.e., the intersection of the original “guiding” resonance with a weaker resonance. The

phenomenon suggested by our results is a *multipulse intermittency* in diffusion near double resonances. This intermittency means that the slowly diffusing trajectories temporarily become “alive” and exhibit several irregular transients before they cross the resonance junction along the stronger resonance. As it follows from the results in ref. 16, the measure of initial conditions exhibiting this phenomenon is algebraic in ε , hence the resulting multipulse intermittency should be numerically observable.

Finally, we note that, although the intersection of a weaker and a stronger resonance is a much more frequent occurrence in phase space, the dynamics near strong–strong resonance junctions is also of great interest. Our methods cannot be applied directly in this situation since the auxiliary perturbation parameter μ in the corresponding pendulum Hamiltonian (6) is no longer small. Nevertheless, since the types of structures we described in this paper are structurally stable, they are expected to survive for somewhat larger μ values as well. This suggests that the remnants of the multipulse intermittency we described here continue to exist near the intersection of equally strong resonances. We believe that this question deserves further study and can be answered affirmatively by applying numerical continuation techniques to given examples.

ACKNOWLEDGMENTS

The author is grateful to V. I. Arnold, C. G. Ragazzo, and S. Wiggins for helpful discussions on the subject of this paper, and to the anonymous referees for useful comments. In addition, he is indebted to G. Gallavotti for several insightful remarks and for pointing out a crucial error in an earlier version of the manuscript. This work was supported by NSF grant DMS-95011239.

REFERENCES

1. V. I. Arnold, Instability of dynamical systems with several degrees of freedom, *Sov. Math. Doklady* 5:581–585 (1964).
2. V. I. Arnold, V. V. Kozlov, and A. I. Neishtadt, *Dynamical Systems III* (Springer, New York, 1988).
3. V. I. Arnold, Mathematical problems in classical physics, in *Trends and Perspectives in Applied Mathematics*, L. Sirovich, ed. (Springer, New York, 1994), pp. 1–21.
4. G. Benettin and G. Gallavotti, Stability of motions near resonances in quasi-integrable Hamiltonian systems, *J. Stat. Phys.* 44:293 (1986).
5. L. Chierchia and G. Gallavotti, Drift and diffusion in phase space, *Ann. IHP Phys. Theor.* 160:1–144 (1994).
6. L. Chierchia, Arnold instability for nearly-integrable analytic Hamiltonian systems, preprint (1995).

7. L. Chierchia, Non-degenerate "Arnold diffusion," preprint (1996).
8. B. V. Chirikov, A universal instability of many-dimensional oscillator systems, *Phys. Rep.* **52**:263–379 (1979).
9. N. Fenichel, Persistence and smoothness of invariant manifolds for flows, *Ind. Univ. Math. J* **21**:193–225 (1971).
10. N. Fenichel, Geometric singular perturbation theory for ordinary differential equations, *J. Diff. Eqs.* **31**:53–98 (1979).
11. E. V. Gaidukov, Asymptotic geodesics on a Riemannian manifold nonhomeomorphic to the sphere, *Sov. Math. Doklady* **7**:1033–1035 (1966).
12. G. Gallavotti, Twistless KAM tori, quasi-flat homoclinic intersections, and other cancellations in the perturbation series of certain completely integrable Hamiltonian systems: A review, *Rev. Math. Phys.* **6**:340–411 (1994).
13. S. M. Grafl, On the conservation of hyperbolic invariant tori for Hamiltonian systems, *J. Diff. Eqs.* **15**:1–69 (1974).
14. G. Haller and S. Wiggins, Orbits homoclinic to resonances: The Hamiltonian case, *Physica D* **66**:298–346 (1993).
15. G. Haller, Multi-pulse homoclinic phenomena in resonant Hamiltonian systems, Ph.D. Thesis, Caltech (1993).
16. G. Haller and S. Wiggins, N -pulse homoclinic orbits in perturbations of resonant Hamiltonian systems, *Arch. Rat. Mech. Anal.* **130**:25–101 (1995).
17. G. Haller, Diffusion near intersecting resonances in Hamiltonian systems, *Phys. Lett. A* **200**:34–42 (1995).
18. G. Haller, Multi-pulse homoclinic for multi-dimensional systems, with an application to the discretized, perturbed NLS, *Commun. Math. Phys.*, submitted.
19. P. Holmes and J. Marsden, Horseshoes in perturbations of Hamiltonian systems with two degrees of freedom, *Commun. Math. Phys.* **82**:523–544 (1982).
20. P. Holmes and J. Marsden, Melnikov's method and Arnold diffusion for perturbations of integrable Hamiltonian systems, *J. Math. Phys.* **23**:669–675 (1982).
21. C. K. R. T. Jones and N. Kopell, Tracking invariant manifolds with differential forms in singularly perturbed systems, *J. Diff. Eqs.* **108**:64–88 (1994).
22. C. K. R. T. Jones, T. Kaper, and N. Kopell, ELESE: The exchange lemma with exponentially small error, *SIAM J. Math. Anal.*, to appear.
23. N. Kopell, Invariant manifolds and the initialization problem in some atmospheric equations, *Physica D* **14**:203–215 (1985).
24. G. Kovačič and S. Wiggins, Orbits homoclinic to resonances with an application to the damped and forced sine-Gordon equation, *Physica D* **57**:185–225 (1992).
25. J. Laskar, Global dynamics and diffusion, *Physica D* **67**:257–281 (1993).
26. A. J. Lichtenberg and M. A. Leiberman, *Regular and Chaotic Dynamics*, 2nd ed. (Springer, New York, 1992).
27. P. Lochak, Effective speed of Arnold diffusion and small denominators, *Phys. Lett. A* **143**:39–42 (1990).
28. J. Moser, Convergent series expansions for quasi-periodic motions, *Math. Ann.* **169**:136–176 (1967).
29. S. Smale, Diffeomorphisms with many periodic points, in *Differential and Combinatorial Topology*, S. S. Carns, ed. (Princeton University Press, Princeton, New Jersey, 1963), p. 63.
30. S. K. Tin, On the dynamics of tangent spaces near a normally hyperbolic invariant manifold, Ph.D. Thesis, Brown University (1994).
31. D. V. Treshchev, The mechanism of destruction of resonance tori of Hamiltonian systems, *Math. USSR Sbornik* **68**:181–202 (1991).

32. S. Wiggins, *Normally Hyperbolic Manifolds in Dynamical Systems* (Springer, New York, 1994).
33. E. Zehnder, Homoclinic points near elliptic fixed points, *Commun. Pure Appl. Math.* **26**:131–182 (1973).
34. E. Zehnder, Generalized implicit function theorems with applications to small divisor problems I, *Commun. Pure Appl. Math.* **28**:91–140 (1975).
35. E. Zehnder, Generalized implicit function theorems with applications to small divisor problems II, *Commun. Pure Appl. Math.* **29**:49–111 (1976).